理學博士學位論文

파킨슨병 초파리모델에서 Glutathione S-Transferase Omega 의 기능에 대한 연구

The Functional Study of Glutathione S-Transferase Omega in *Drosophila* Model of Parkinson Disease

2012年 8月

서울大學校 大學院

生命科學部

金 起 永

파킨슨병 초파리모델에서 Glutathione S-Transferase Omega 의 기능에 대한 연구

指導敎授 任 正 彬

이 論文을 理學博士 學位論文으로 提出함

2012年 5月

서울大學校 大學院

生命科學部

金 起 永

金起永의 理學博士 學位論文을 認准함

2012年 6月

委 員 長 _____

副委員長 _____

委 員 _____

委 員 _____

委 員 _____

The Functional Study of Glutathione S-Transferase Omega

in *Drosophila* Model of Parkinson Disease

A dissertation submitted in partial fulfillment
of the requirements for the degree of
DOCTOR OF PHILOSOPHY

to the Faculty of the
School of Biological Sciences

at
SEOUL NATIONAL UNIVERSITY

by
Kiyoung Kim

Date Approved

June 21, 2012

Deog Su Hwang

Yoon Jaeseung

Jaekyoo Chung

Won-jae Lee

The Functional Study of Glutathione S-Transferase Omega in *Drosophila* Model of Parkinson Disease

by

Kiyoung Kim

Advisor:

Prof. Jeongbin Yim, Ph. D.

A Thesis Submitted in Partial Fulfillment of the Requirements for the Degree of Doctor of Philosophy

August, 2012

School of Biological Sciences
Graduate School
Seoul National University

ABSTRACT

Parkinson disease (PD) is the most common progressive neurodegenerative movement disorder. Mutations in autosomal recessively inherited genes, *parkin*, *PINK1*, *DJ-1*, lead to early onset parkinsonism. The main symptoms of PD result from the selectively and extensively loss of dopaminergic neurons in the substantia nigra of the midbrain. Recent researches have shown that parkin and PINK1 play important roles in the regulation of mitochondrial functions and dynamics. A loss-of-function mutation in the gene *parkin* or *PINK1* displays several defective phenotypes, including increased apoptotic cell death, oxidative stress and aggregation of abnormal proteins. Despite several intensive studies, the exact molecular pathogenesis of PD remains unknown.

Glutathione S-transfearses (GSTs), one of the largest gene families of multi-functional enzyme, involved in the detoxification of endogenous and exogenous substrates. A new class of GST, GST Omega (GSTO) has a glutathione-dependent thiol transferase and glutathione-dependent dehydroascorbate reductase activity, reminiscent of thioredoxins and glutaredoxins. *GSTO* gene has been shown to be associated with the age-at-onset of PD. Moreover, GSTO protects cells against oxidative stress that have been implicated in the pathology of neurodegenerative disease. Although there have been studies regarding the function of GSTOs in neurodegenerative

disease, little is known about the role of GSTO in the progression of PD.

Here, we report that restoration of *Drosophila* GSTO1 (DmGSTO1), which is down-regulated in *parkin* mutants, alleviates some of the *parkin* pathogenic phenotypes and that the loss of *DmGSTO1* function enhances *parkin* mutant phenotypes. We further identified the ATP synthase β subunit, which is a core component of the mitochondrial F_1F_0-ATP synthase (Complex V), as a novel *in vivo* target of DmGSTO1. We found that glutathionylation of the ATP synthase β subunit is rescued by DmGSTO1 and that the expression of DmGSTO1 partially restores the activity and assembly of the mitochondrial F_1F_0-ATP synthase in *parkin* mutants. Additionally, we show that glutathionylation of ATP synthase β subunit is decreased in $PINK1^{B9}$ mutants and that up-regulation of DmGSTO1 rescues the defective phenotypes in $PINK1^{B9}$ mutants. These results suggest that DmGSTO1 interacts with the PINK1/Parkin pathway in *Drosophila*. Our results suggest a novel mechanism for the protective role of DmGSTO1in *parkin* mutants, through the regulation of ATP synthase activity, and provide insight into potential therapies for PD neurodegeneration.

Keywords: Parkinson disease; Glutathione S-Transferase Omega (GSTO); Glutathionylation; Mitochondria; Mitochondrial F_1F_0-ATP synthase; ATP synthase β subunit; *Drosophila melanogaster*

Student number: 2004-20498

CONTENTS

III. Results

LIST OF FIGURES AND TABLES

ABBREVIATIONS

ANOVA	analysis of variance
AsA	ascorbate
ATP	adenosine triphosphate
BisTris	2-[bis(2-hydroxyethyl)amino]-2-(hydroxymethyl)propane-1, 3-diol
DA	dopaminergic neuron
DHA	dehydroascorbate
DHAR	dehydroascorbate reductase
ER	endoplasmic reticulum
Foxo-like	fork head box-like
Grx	glutaredoxin
GSH	glutathione
GST	glutathione s-transferase
GSTO	glutathione s-transferase omega
GSTP	glutathione s-transferase pi
GSTS	glutathione s-transferase sigma
HPLC	high-performance liquid chromatography
HSP	heat shock protein
IFM	indirect flight muscle
JNK	*c*-Jun N-terminal kinase
LC-MS/MS	liquid chromatography-tandem mass spectrometry
MALDI-TOF	matrix-assisted laser desorption/ionization time-of-flight mass spectrometer
Mito-GFP	*mitochondrial-green fluorescent protein*
NF-κB-like	nuclear factor kappa B-like

PD	Parkinson disease
PINK1	PTEN-induced putative kinase 1
RT-PCR	polymerase chain reaction after reverse transcription of RNA
S.D.	standard deviation
SDS-PAGE	sodiumdodecylsulfate polyacrylamide gel electrophoresis
TH	*tyrosine hydroxylase*
Trx	thioredoxin
Tub	*tubulin*
TUNEL	terminal deoxynucleotidyl transferase mediated-biotinylated UTP nick end labeling
UAS	upstream activation sequence
UPR	unfolded protein response
WT	wild type

I. Introduction

1. Parkinson disease

Parkinson disease (PD) is a progressive neurodegenerative disorder characterized by the degeneration of dopaminergic (DA) neurons (Figure 1). Previous reports suggested that mitochondrial dysfunction, oxidative stress, and ER stress induced by the aggregation of abnormal proteins can contribute to the pathogenesis of PD (Dawson, 2003; Abou-Sleiman *et al*., 2006). Most case of PD occur sporadically with unknown mechanism, but mutations in several genes, such as *parkin*, *PINK1*, *LRRK2*, *DJ-1* and *α-synuclein*, have been associated with genetic forms of PD. However, the molecular mechanisms of PD pathogenesis have not yet been fully elucidated. A loss-of-function mutation in the *parkin* gene is a major cause of autosomal recessive, early onset PD. Parkin acts as an E3 ubiquitin protein ligase in the proteasome-medicated protein degradation (Figure 2). Therefore, the substrates of parkin for proteasomal degradation are accumulated in *parkin* mutations. Several putative substrates have been founded for parkin on the basis of *in vitro* cell culture system, including synphilin-1, α-synuclein, the parkin-associated endothelin receptor-like receptor (Pael-R), synaptotagmin XI, CDCrel-1, cyclin E, and α/β-tubulin (Chung *et al.*, 2001; Shimura *et al.*, 2001; Imai *et al.*, 2001; Zhang *et al.*, 2000; Staropoli *et al.*, 2003; Ren *et al.*, 2003). However, it is not clear whether parkin regulates protein degradation of endogenous substrates *in vivo*. Recent researches have shown that parkin plays an important role in the protection of mitochondrial integrity.

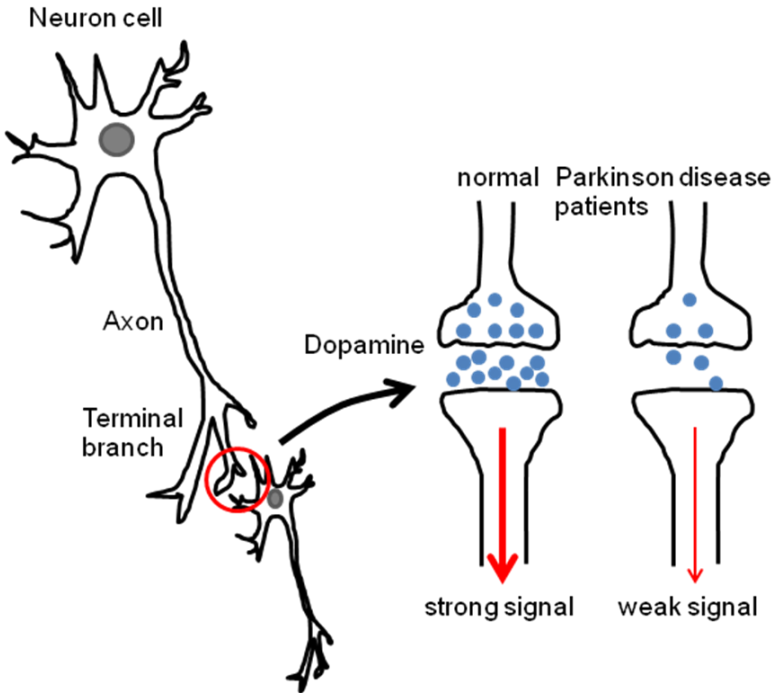

Figure 1. Dopamine depletion is the hallmark of Parkinson disease.

Parkinson disease is a progressive disease caused by the decreased production of dopamine in the substantia nigra pars compacta. The neurotransmitter, dopamine, is responsible for the communication of neurons that control muscle motion.

Overexpression of *parkin* increased mitochondrial membrane potential, the expression of mitochondrial complex I subunits (Kuroda *et al.*, 2006). Mutation of parkin in *Drosophila* results in mitochondrial abnormalities and apoptosis in thorax muscles and increased sensitivity to oxidative stress (Greene *et al.*, 2003; Pesah *et al.*, 2004). Moreover, *parkin* null mice display increased levels of oxidative stress, lipid oxidation, and reduced mitochondrial respiratory (Palacino et al., 2004).

PINK1 is a putative serine/threonine kinase, which is predominantly localized at the inner mitochondrial membrane (Figure 2) (Valente *et al*., 2004). Recent studies show that PINK1 plays an important role in various biological processes, including oxidative stress, calcium homeostasis, mitochondrial dynamic and mitochondrial metabolism. Mutations in the *PINK1* gene contributed to the disease because of the loss of kinase activity that lead to morphological defects of mitochondria and impaired energy metabolism (Park *et al.*, 2006; Deng *et al.*, 2008; Poole *et al.*, 2008; Yang *et al.*, 2008; Clark *et al.*, 2006). *PINK1* mutant in *Drosophila* exhibit locomotor defect and male sterility (Park *et al*., 2006; Clark *et al*., 2006). Similar to *parkin* mutant in *Drosophila*, the mitochondria were swollen with reduced ATP levels. Dopaminergic neurons were significantly reduced in *PINK1* mutants. Furthermore, overexpression of parkin alleviated PINK1 loss-of-function defective phenotypes, whereas overexpression of PINK1 had no effect on parkin loss-of-function phenotypes. Thus, parkin and PINK1 function in a common pathway. Finally, PINK1/Parkin pathway plays a critical role in maintaining mitochondrial function by regulating several mitochondrial processes. However, it remains unclear which of these processes are directly regulated by PINK1/Parkin pathway.

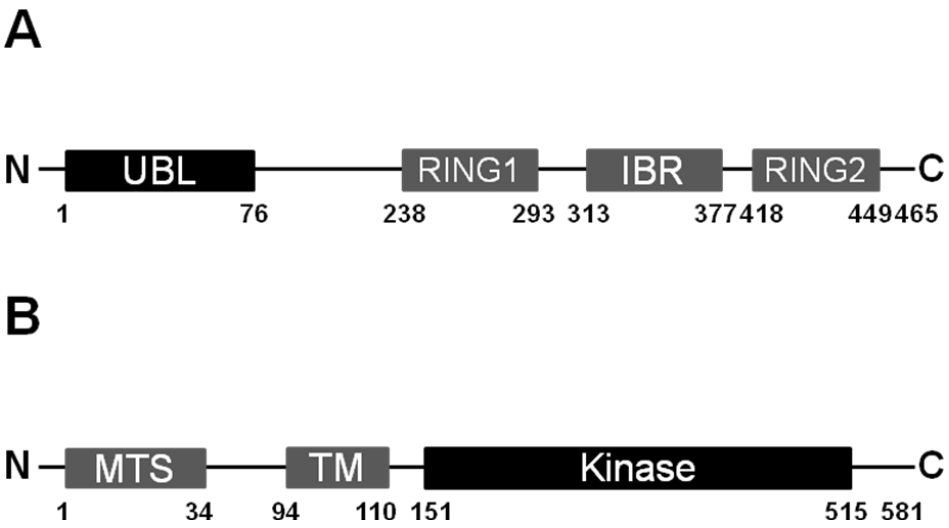

Figure 2. Schematic representation of the domain composition of Parkin and PINK1

(A) Domain structure of parkin. Domains are arranged from N-terminus to C-terminus. UBL, ubiquitin-like domain; RING1, RING-finger motif 1; IBR, in between RING-finger motif; RING2, RING-finger motif 2. (B) Domain structure of PINK1. MTS, mitochondrial targeting sequence; TM, putative transmembrane domain; Kinase, serine/threonine kinase domain.

2. Glutathione S-Transferase Omega

Glutathione S-transferases (GSTs) constitute a superfamily of enzymes that are grouped into at least 10 classes; some superfamily members are known to be involved in cell defense mechanisms (Hayes *et al.*, 2005; Sheehan *et al.*, 2001). In mammals, the cytosolic GSTs are homodimers or heterodimers and have been classified into eight distinct gene classes, Alpha, Mu, Pi, Theta, Sigma, Zeta, Kappa and Omega, according to substrate specificity and their structural, catalytic properties. GSTs are expressed at several levels in animal tissues but are inducible by various substances, carcinogens, therapeutic drugs, and products of oxidative stress. Several functions of GSTs have been discovered; binding of hydrophobic ligands, gene regulation, and apoptosis. The N-terminal region of GSTs contains the GSH-binding site and is classified as part of thioredoxin fold, which includes glutaredoxin, disulfide-bond formation mediator (Murzin *et al*., 1995). The substrate-binding site is located in the C-terminal region.

Drosophila GST superfamily consists of 36 genes which encode 41 GST proteins. In fact six classes, Theta, Sigma, Zeta, Delta, Epsilon and Omega, appear to exist in *Drosophila*. Omega class in *Drosophila* has four genes that encode five proteins. The *Drosophila* GST genes are located on chromosomes X, 2 and 3 (Tu *et al*., 2005). The distribution of GST genes on the chromosomes suggests that these GSTs originated from duplication events. The gene duplication events in *Drosophila* gave rise to differentially expressed GST isoforms and generated various members with different function.

A new class of GSTs, Omega, has been described based on sequence alignments GST Omegas (GSTOs) have a 19 amino acid extension in N-terminus (Board *et al.*,

2000). The active sites of GST Omega have a unique cysteine residue that can form a disulfide bond with GSH, whereas other eukaryotic GSTs have tyrosine or serine residues in their active sites (Sheehan *et al.*, 2001). The biological functions of several GSTOs have been determined. Human GSTO1-1 modulates calcium channels (Dulhunty *et al.*, 2001), has a role in the activation of interleukin-1β (Laliberte *et al.*, 2003), and interacts with a serine protease inhibitor (Yin *et al.*, 2005). Recently, our group reported that one of the four *GSTO* genes in *Drosophila*, *CG6781*, is the structural gene of the *Drosophila* eye color mutant, *sepia*, which encodes pyrimidodiazepine synthase, a key enzyme in the drosopterin biosynthetic pathway (Kim *et al.*, 2006). In human, GSTOs are mapped to the linkage region correlated with the age at onset of Alzheimer disease (Li *et al.*, 2003). Variations in human *GSTO1* genes that modify the age at onset of Alzheimer and Parkinson diseases have been reported (Li *et al.*, 2006). Pallanck's group (Greene *et al.*, 2005; Whitworth *et al.*, 2005; Trinh *et al.*, 2008) reported that expression of *Drosophila melanogaster* GST Sigma 1 (DmGSTS1), which is another member of the GST family in *Drosophila*, suppresses the phenotypes of *parkin* mutants and α-synuclein-expressing mutants.

3. Glutathionylation

Glutathionylation is a reversible post-translational modification of cysteine residues by addition of GSH (Townsend *et al.*, 2009). Glutathionylation is regulated by glutaredoxins, thioltransferases, and glutathione S-transferase, members of the thiol-disulfide oxidoreductase family that contain a thioredoxin fold. Proteins involved in the reduction of oxidized cysteine residues include thioredoxin and glutaredoxin.

Thioredoxin can reduce disulfide bonds. Glutaredoxin not only deglutathionylates some proteins but has also been shown to catalyze glutathionylation of several proteins (Figure 3) (Starke *et al.*, 2003). Glutathionylation can have a variety of effects on protein function. Reversible post-translational modification, such as glutathionylation, may have a dual function of protection against protein thiol oxidation and modulation of protein function. Many proteins (Table 1), such as Neurofibromatosis-related protein-1, c-jun, NF-κB, tubulin, actin, IKKβ, STAT3, and IkBα, have been found to be glutathionylated and protein activity is altered by glutathionylation (Shelton and Mieyal, 2008). Glutathionylation of several proteins was found to be involved in physiological processes, differentiation, transcriptional activation, cytoskeletal function, protein folding, and metabolism. Glutathionylation is emerging as a post-translational modification that potentially plays an important regulatory role in signal transduction pathway. The increasing evidence of protein functional changes resulting from glutathionylation, and the growing number of glutathionylated proteins *in vitro* support this as an important scientific field. However, the molecular mechanism of protein-glutathionylation is not fully elucidated.

4. Mitochondrial F_1F_0-ATP synthase

The F_1F_0-ATP synthase is localized in plasma membranes of bacteria, mitochondrial inner membranes of eukaryotic cells, and chloroplast thylakoid membranes of plants. The mitochondrial F_1F_0-ATP synthase (Complex V) is a membrane protein complex that catalyzes the synthesis of ATP coupled to the hydrogen ion gradient generated in the respiratory chain (Figure 4).

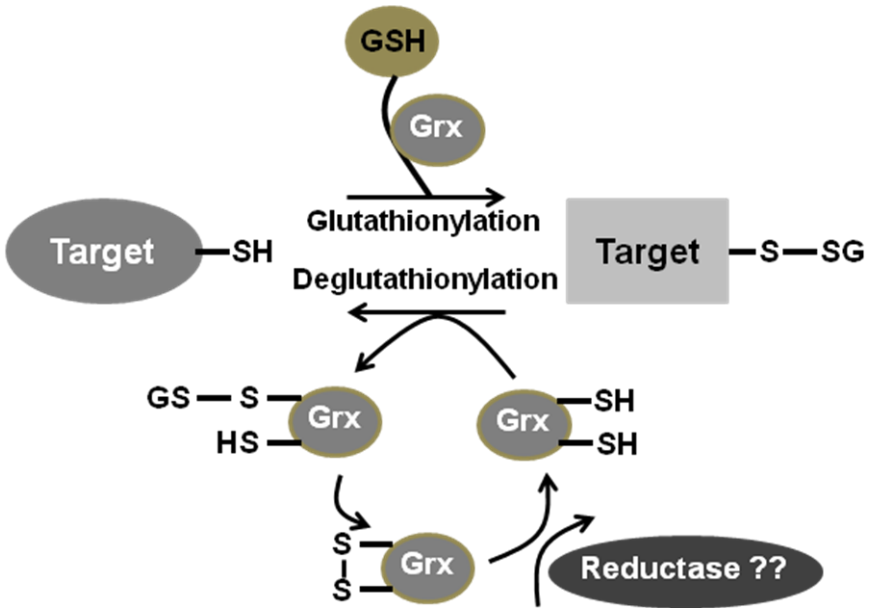

Figure 3. Glutaredoxin-dependent mechanism for glutathionylation

Glutaredoxin could catalyze glutathionylation in the presence of GSH. The reverse reaction, deglutathionylation, is also catalyzed by glutaredoxin. Then, the resulting disulfide bond in glutaredoxin is reduced by specific-reductase.

Target protein	Function
Actin	cell adhesion, interaction
Tubulin	mitosis, cell movement
Complex V	mitochondrial redox balance
ATPase	mitochondrial redox balance
MEKK1	kinase
PTP1B	phosphatase
PTEN	phosphatase
NF-κB	transcription factor
p53	transcription factor
HSP65, 70	protein chaperone
20S proteosome	protein stability
Ubiquitin conjugating enzyme	protein stability

Table 1. Glutathionylated proteins

The several analysis suggest that the glutathionylation of proteins may affect very specific cellular function. The proteins were identified as targets in cell culture system and *in vitro*. However, the functions of glutathionylation are not yet fully elucidated *in vivo*.

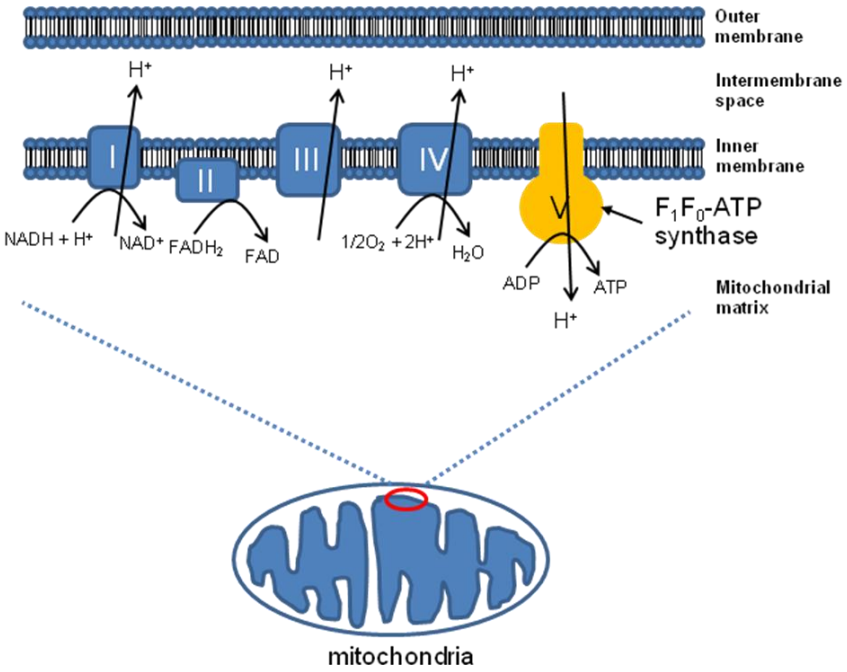

Figure 4. F_1F_0-ATP synthase at the mitochondrial inner membrane

The electrochemical H^+ gradient and a high energy electron are passed along an electron transport chain. The F_1F_0-ATP synthase pumps H^+ out to the matrix between the mitochondrial membranes. The gradient created by this high concentration of H^+ outside of the inner membrane drives H^+ back through the inner membrane, through F_1F_0-ATP synthase. The enzymatic activity of F_1F_0-ATP synthase synthesizes ATP from ADP.

The mitochondrial ATP synthase is a large multi-protein complex composed of sixteen different subunits that form catalytic F_1 domain connected with the proton-translocating transmembrane F_0 domain (Collinson et al., 1996). The most of ATP synthase subunits are subject to nuclear transcription and translocate to the mitochondria, and assembly into a large multi-protein complex in the inner membrane. ATP synthase activity is important to maintain mitochondrial membrane potential and to generate ATP through oxidative phosphorylation (Celotto *et al.*, 2006).

The *ATP6*, mitochondrial F_1F_0-ATP synthase a subunit, mutation was discovered in *Drosophila*. This mutant flies exhibit several defective phenotypes including reduced locomotive activity, muscle degeneration, and neuronal dysfunction (Celotto *et al.*, 2006). Previously studies indicate mitochondrial F_1F_0-ATP synthase may play a role in neurodegenerative diseases, Huntington's disease (HD) (Wang *et al.*, 2009).

5. Purpose of this study

To elucidate the protective role of GSTO in neurodegenerative diseases, we investigated the biological function of *D. melanogaster* GSTO (DmGSTO) in a *Drosophila* model of PD. We found that one of the DmGSTOs, DmGSTO1, is able to rescue some phenotypes of *parkin* mutants, including the degeneration of DA neurons and muscle. The ability of DmGSTO1 to rescue these phenotypes was dependent on the catalytic activity of DmGSTO1. Furthermore, tubulin accumulation and ER stress caused by the *parkin* mutation were also significantly reduced by ectopic expression of *DmGSTO1*. We discovered that the *Drosophila* ATP synthase β subunit (Pena and

Garesse, 1993) is a novel target of DmGSTO1, and up-regulation of DmGSTO1 restored glutathionylation levels of the ATP synthase β subunit in *parkin* mutants. The mitochondrial F_1F_0-ATP synthase is a membrane protein complex that couples the synthesis of ATP to the hydrogen ion gradient generated by the respiratory chain (Calpaldi and Aggeler, 2002; Cross and Muller, 2004). The up-regulation of DmGSTO1 also restored ATP synthase activity, complex assembly, and ATP levels in *parkin* mutants. Our findings suggest that DmGSTO1 plays a protective role in *parkin* mutations by regulating mitochondrial ATP synthase activity.

II. Materials and Methods

1. *Drosophila* stocks

w^{1118} and *Oregon-R* were used as a control strain. The UAS-*mito*GFP line was a gift from H. J. Bellen (Baylor College of Medicine, Houston, TX) (Verstreken *et al.*, 2005). We generated four transgenic lines: *DmGSTO1A*, *DmGSTO1B*, *DmGSTO1A*^{C31A}, and *CG6662*. The coding sequences for these four genes were amplified by PCR. The four PCR products were ligated into the pUAST expression vector and introduced into the germ line by microinjection. All PCR products were confirmed by DNA sequencing. *Drosophila* stocks were maintained in standard food conditions at 25 ℃. The *parkin* null mutant line, *park*^{1}, and *PINK*^{B9} were gifts from J. Chung (Seoul National University) (Cha *et al.*, 2005; Park *et al.*, 2006). The *TH*-Gal4 line was gift from S. Birman (CNRS-Université de le Méditerranée) (Friggi-Grelin *et al.*, 2003). The *Tub*-Gal4 fly line and the *24B*-Gal4 line were obtained from Bloomington Stock Center. We obtained the ATP synthase β subunit RNAi lines, CG11154R-1 and R-3, from the NIG-FLY stock center (National Institute of Genetics, Mishima, Japan).

2. Generation of *DmGSTO1*^{null} mutant by Imprecise excision

To generate *DmGSTO1* mutants, we obtained the *GE26508 P*-element insertion line from the GenExel *Drosophila* library (KAIST, Daejeon, Korea). The *P*-element was mobilized using transposase, and *GE26508* was imprecisely excised to generate *DmGSTO1*^{null}. A loss-of-function mutant, *DmGSTO1*^{null}, whose deletion range covers

the open reading frame of DmGSTO1 transcript was confirmed by genomic PCR. PCR was performed using DmGSTO1 specific primers with the Dys-2 forward sequence being 5'-GCC GGC AAT GCA AAC TAC GAT CTG-3' and the Dys-3 reverse sequence being 5'-AAT CCC GAG CAG CTG GTT GAC ACC-3', to obtain a product of 4.1 kb.

3. Preparation of Genomic DNA

Thirty to Fifty frozen adult flies were grinded in 400 µl of buffer A (100 mM Tris-Cl pH 7.5, 100 mM EDTA, 100 mM NaCl, 0.5% SDS) with a disposable tissue grinder, and incubated at 65 ℃ for 30 minutes. Add 800 µl LiCl/KAc Solution into the tube and incubate it on ice for at least 10 minutes. After centrifugation at 13,500 rpm for 15 minutes, 1 ml of the supernatant was transferred into a new tube. 600 µl of isopropanol was added to precipitate the DNA, and the genomic DNA pellet was recovered by centrifugation at 13,500 rpm for 15 minutes at 4℃. After the supernatant was removed, genomic DNA pellet was washed with 70% ethanol and air-dried. The pellet was resuspended in 100 µl of TE or DW.

4. Inverse PCR

One to five µg of genomic DNA was fully digested with *Sau3A*I, and the DNA fragments were self-ligated. After precipitation, the ligated DNAs were used in PCR reaction. For 5’ end of p[EP] vector, PCR was performed using specific primers with the forward sequence being 5’-ACT GTG CGT TAG GTC CTG TTC ATT GTT-3’

(Plac4) and the reverse sequence being 5'-CAC CCA AGG CTC TGC TCC CAC AAT-3' (Plac1). For 3' end of p[EP], PCR was performed using specific primers with the forward sequence being 5'-CAA TCA TAT CGC TGT CTC ACT CA-3' (Pry4) and the reverse sequence being 5'-CCT TAG CAT GTC CGT GGG GTT TGA AT-3' (Pry1). PCR products were ligated into the pGEM-T easy vector (Promega) and confirmed by DNA sequencing.

5. Exposure to Paraquat

One- to two-day-old male flies were staved for 5 h and then kept in vials with 3M filter paper soaked with 20 mM paraquat (Methyl Viologen, Sigma-Aldrich) in 5% sucrose. Files were kept in the dark at all times.

6. Ascorbic acid and Dehydroascorbic acid Content

To measure ascorbic acid content, about 30 male flies were homogenized in 200 µl of cold 5% metaphosphoric acid and centrifuged at 25,000 X g. The ascorbic acid contents were quantified using reverse phase HPLC equipped with Waters Model 510 pump, photodiode array detector (Waters 996), and reverse phase Inertsil ODS-3 C18 column (particle size 5 µm, 4.5 x 250 mm, GL Sciences Inc, Japan). The material was eluted isocratically with 0.2 M KH_2PO_4/H_3PO_4 in 7% methanol pH 3.0 containing 2 mM EDTA at flow rate of 1 ml/min. Ascorbic acid was monitored by the absorbance at 245 nm.

7. Immunoblot Analysis

Protein extracts for immunoblot analysis were prepared by homogenizing 10 fly thoraces from 3-day-old male flies in lysis buffer (50mM Tris-HCl, pH 7.5, 150 mM NaCl, and 0.5% Nonidet P-40) containing a protease inhibitor mixture (1X; Calbiochem-Merck4Biosciences). Total protein (20 μg) was separated by 8 or 10% SDS-PAGE and transferred to PVDF membranes (Millipore). Membranes were blocked by Tris-buffered saline (TBS) with 4% nonfat dry milk or 4% BSA for 1 h. We used the following primary antibodies: rabbit anti-phospho-JNK (1:1,000; Promega), rabbit anti-JNK (1:1,000; Santa Cruz Biotechnology, Inc. (Santa Cruz, CA)), rabbit anti-β-actin (1:5,000; Sigma-Aldrich), mouse anti-α-tubulin (1:4,000; Sigma-Aldrich), mouse anti-β-tubulin (1:3,000; Sigma-Aldrich), rabbit anti-phospho-eIF2α Ser-51 (1:1,000; Cell Signaling Technology), rabbit anti-eIF2α (1:200; Abcam), rabbit anti-HSP60 (1:1,000; Stressgen Bioreagents, Kampenhout, Belgium), mouse anti-HSP/HSC70 (1:1,000; Stressgen Bioreagents), mouse anti-ATP synthase β subunit (1:20,000; Mitosciences), rabbit anti-prohibitin (1:500; Abcam), and rabbit anti-*Drosophila* ATP synthase β subunit (1:20,000; a kind gift from Rafael Garesse, Universidad Autonoma de Madrid). Detection of the primary antibodies was carried out with HRP-conjugated secondary antibodies and an ECL-Plus detection kit (Amersham Biosciences). Polyclonal antibodies against *Drosophila* GSTO1A were produced by immunizing rabbits with a C-terminal synthetic peptide, ^{231}EFQKSKTLGNPQY^{243}, as the antigen (Abfrontier).

8. Muscle Histology

Muscle section analysis was carried out as described previously (Pesah *et al.*, 2004) with some modifications. For muscle tissue analyses, whole thoraces from 3-day-old male flies were fixed with 4% formaldehyde overnight at 4 ℃. After fixation, the samples were oxidized with 1% OsO4 for 2 h at room temperature and then dehydrated in a series of acetone/water mixtures of increasing acetone concentration (50, 70, 80, 90, and 100% acetone). The samples were embedded in Spurr's resin. The thoraces were then trimmed and sectioned from the transverse side of the thorax. The sections were stained with a toluidine blue dye and observed by light microscopy (Carl Zeiss, Axio Imager A1).

9. Immunohistochemistry and TUNEL Assay

Adult brains and thoraces of 1-, 3-, 5-, and 20-day-old male flies were fixed with 4% formaldehyde in a fixative buffer (100mM PIPES, 1mM EGTA, 1% Triton X-100, and 2 mM MgSO4, pH 6.9) and blocked in a wash buffer (50 mM Tris, 150 mM NaCl, 0.1% Triton X-100, and 0.5 mg/ml BSA, pH 6.8) with 10 mg/ml BSA. The following antibodies were used: rabbit anti-TH (1:100; Pel-freeze), mouse anti-TH (1:100; Immunostar), rabbit anti-phospho-JNK (1:100; Promega), mouse anti-GFP (1:500; Roche Applied Science), and mouse anti-α-tubulin (1:500; Sigma-Aldrich). Alexa 488-conjugated streptavidin (1:100; Invitrogen) was used to identify mitochondria. Rhodamine phalloidin (Invitrogen) was used to visualize actin. All images were obtained on a Carl Zeiss confocal microscope (DE/LSM510 NLO).

For the TUNEL assay, apoptosis in the indirect flight muscles (IFMs) of 3-day-old flies was detected using the *In Situ* Cell Death Detection Kit, Fluorescein (Roche Applied Science).

10. Quantitative RT-PCR and Real-time Quantitative RT-PCR

Total RNA was extracted with TRIzol reagent (Invitrogen), and cDNA was prepared from 2 μg of total RNA using Moloney murine leukemia virus reverse transcriptase (Promega). The PCRs were performed using Ex Taq (Takara Bio, Otsu, Japan) and TaqDNA polymerase (Bioneer, Daejeon, Korea) with a PTC-100 programmable thermal controller (MJ Research). We used the previously reported *Drosophila* GSTO primers for *CG6776*, *CG6662*, *DmGSTO1A*, and *DmGSTO1B* (Kim *et al.*, 2006). The following *dparkin* and *dPINK1* primers were used: *dparkin*-For (CAT ATG AGT TTT ATT TTT AAA TTT ATT GCC ACT TTT GTA C), *dparkin*-Rev (CTC GAG TTA GCC GAA CCA GTG GG), *dPINK1*-For (TTC TGC CAC CAC CGC CCC CAC ACT TC), and *dPINK1*-Rev (CCG CAG CAC ATT GGC AGC GGT GG).

The comparative cycle threshold (*Ct*) method was adapted to estimate transcript levels using an ABI7300 system (Applied Biosystems). The transcript levels were calculated as the relative-fold change over *rp49* mRNA. We used the following primers for α-*tubulin*, and β-*tubulin*: α-*tubulin*-For (ACA ACG AGG CTA TCT ACG ACA TCT), α-*tubulin*-Rev (TTT TCA GTG TTG CAG TGA ATT TTT) (Hoopfer *et al.*, 2008), β-*tubulin*-For (CAA GGC TTC CAA CTC ACA CAC TC), and β-*tubulin*-

Rev (AGG TGG CGG ACA TCT TCA GAC) (Matyunina *et al.*, 2008). The sequences of primer sets used in the PCR reactions are shown in Table 2.

11. Site-directed Mutagenesis and Expression of Mutant Proteins

The DmGSTO1A^{C31A} mutant was generated by site-directed mutagenesis (Cosmo Genetech, Seoul, Korea). Cysteine 31 at the active site was mutated to alanine by changing the TGC codon encoding cysteine 31 to GCC. Mutated DNA was sequenced to confirm the single codon change. The DmGSTO1A^{C31A} mutant was expressed in *Escherichia coli* strain BL21 after cloning the cDNA into a pET15b expression vector (Novagen-Merck4Biosciences).

12. *in vitro* Glutathionylation Assay

Recombinant ATP synthase β subunit (5 μg) was incubated at 37 ℃ in 50 mM potassium phosphate (pH 7.6), and 10 mM GSH in the presence of either recombinant DmGSTO1A or DmGSTO1B protein. After 30 min, the samples were placed on ice, and 5X nonreducing SDS loading buffer was added to the mixtures. Samples were separated by 12% SDS-PAGE, transferred, and probed with mouse anti-GSH (1:1,000; ViroGen Corp.) and rabbit anti-*Drosophila* ATP synthase β subunit (1:4,000) antibodies.

Gene	Forward primer (5'-3')	Reverse primer (5'-3')
CG8517	CCGGTGGTTGTGGACTTTCATGC	TATCGACCCGGGCCAATCTCACT
CG8993	ACCCCGCGCATCGAGAGTATTGT	AACCCAGGCCCGGATTTTGTCCT
CG3719	CGACAACCCGGTGATCGTGAACT	ATGACCGCCAGGTCGATCTCGTT
CG13473	TGGCTGCCATGCAGAAGAAGGTC	CCAGGTGGCGAAGAACTCGACAA
Trx-2	GGCAAGCTGGTGGTGCTGGATTT	TCGCATTCGTCCACATCGACCTT
TrxT	ATGGAGAAGCATGCCGGCGTTTA	TTCACTGGACTCGGCGGTCAGAT
Trx-1(dhd)	TGGCATCCGTACGCACCATGAAC	TCCTTGCAGGGACCACACCATGT
Txl	ACCTGCAGTCCGATTGCGATGAG	TCAATCGTGCGGGGCTGGTTAAT
Trxr-1	TCAACTGGGTGACCCGTGTGGAT	ACGAAGGTCTGGGCGGTGATTGT
Trxr-2	TTCCCTTCCTGGGCACCACAATC	GAAAACGTCGCTGCCGTCCATTT
CG10157	CCATGACATTGCCCAATCCCTCA	TGGCCGTTTCCTTGCCGTACTTC
Clot	CCGGTGATACACGATGCGCTGAA	CAGATGCGTGTTGGGATCCTTGC
Grx-1	AATCAGCGGCAACAAGGTGGTGA	AAGAACCGCCTGGATCTCGTTGC
CG6523	TGGAGGAACGCCTAAAGGCCCTA	ACAATGCCGATGAGCTGCTTGGA
CG6852	ACGATGGCCAAAGAGCCCTTCAA	CATCGATAAAGACGCGGGGAACC

Table 2. Primers used for real-time quantitative RT-PCR

The putative glutathionylating enzymes are conserved in *Drosophila*. There are eleven *thioredoxin* homologue genes and four *glutaredoxin* homologue genes.

13. Immunoprecipitation and Glutathionylation Assay

Thoraces from 3-day-old male flies were homogenized in lysis buffer containing 1X protease inhibitor mixture (Calbiochem-Merck4Biosciences). Thorax lysates were incubated with mouse anti-GSH antibodies (ViroGen) for 2 h at 4 ℃ and incubated overnight with 60 μl of a solution of 50% protein G-Sepharose beads (Amersham Biosciences) at 4 ℃. The resins were collected by centrifugation at 1,000 X *g* for 20 s. Bound proteins, which were glutathionylated, were eluted by boiling in a 2X non-reducing SDS loading buffer for 5 min. Materials were subjected to SDS-PAGE and visualized with Coomassie Blue or silver staining.

After immunoprecipitation with mouse anti-GSH antibodies (ViroGen), proteins bound to resins were separated by 8% SDSPAGE and transferred to PVDF membranes (Millipore) for the glutathionylation assay. Western blot analysis was carried out with rabbit anti-*Drosophila* ATP synthase β subunit antibodies (1:4,000). Signals were detected by HRP-conjugated secondary antibodies.

14. Mitochondrial ATP synthase Activity Assay

To isolate mitochondria from fly thoraces, a mitochondria isolation kit (Pierce) was used according to the manufacturer's protocol. Freshly prepared total mitochondrial protein was used for the ATP synthase activity assay.

ATP synthase activity was measured by ATP hydrolysis using a spectrophotometric method described previously (Rosing *et al.*, 1975). ATP synthase was assayed in 20mM Hepes (pH 7.5), 5mM KCl, 5mM MgCl2, 5 mM KCN, 2.5 mM

phosphoenolpyruvate (Sigma-Aldrich), 15 units of pyruvate kinase (Sigma-Aldrich), 15 units of lactate dehydrogenase (Sigma-Aldrich), 300 µM NADH (Sigma-Aldrich), and 20 µg of total mitochondrial proteins. After 2 min of preincubation at 37 ℃, the reaction was initiated by the addition of 2 mM ATP. The initial velocity of the reaction was followed for 2 min at 340 nm at 37 ℃. The molar extinction coefficient of NADH is 6220 M^{-1}.

15. ATP Assay

Five thoraces from 3-day-old male flies were homogenized in 100 µl of 1X reporter lysis buffer (Promega) on ice. The homogenized samples were quickly frozen in liquid nitrogen to inhibit ATP synthase activity. The frozen samples were boiled for 8 min to destroy endogenous ATP synthase and then centrifuged at 20,000 X *g* for 15 min. ATP was quantified in the supernatant using the ATP bioluminescent assay kit (Sigma-Aldrich) according to the manufacturer's protocol.

16. Blue Native Electrophoresis

Mitochondria were isolated from 3-day-old male fly thoraces using the mitochondrial isolation kit (Pierce). Mitochondrial proteins (10 µg) were dissolved in NativePAGE™ sample buffer (Invitrogen), 1% digitonin (Invitrogen), and 2% dodecylmaltoside (Invitrogen). Samples were incubated for 15 min on ice and centrifuged at 12,000 X *g* for 25 min. Blue native electrophoresis was performed on NativePAGE™ Novex 3–12% BisTris gels (Invitrogen).

III. Results

1. *DmGSTO1* mutants are sensitive to oxidative stress.

We previously reported that there are four different *GSTO* genes in *D. melanogaster*: *CG6781* (*sepia*), *CG6776*, *CG6673*, and *CG6662*. *CG6781* is the structural gene for *sepia*, which encodes pyrimidodiazepine synthase and is expressed exclusively in *Drosophila* heads (Kim *et al.*, 2006). *CG6673* is also called *D. melanogaster* GSTO1 (DmGSTO1) and has the highest thiol transferase and DHA reductase activity among the *GSTO* genes, reminiscent of thioredoxin and glutaredoxin (Kim *et al.*, 2006). *CG6776* responds to heat stress in *Drosophila* (Sørensen *et al.*, 2005). Although the function of *CG6662* is not known, *CG6662* transcripts are primarily expressed in the ovary and testes (Walters *et al.*, 2009). Thus, we focused our study on *CG6673* (*DmGSTO1*) and excluded other *Drosophila GSTO* genes.

We generated both loss-of-function and gain-of-function *DmGSTO1* mutant flies. Because *DmGSTO1* encodes two alternatively spliced transcripts, A and B, we created both DmGSTO1A- and DmGSTO1B-overexpressing fly lines. Loss-of-function mutant $DmGSTO1^{null}$ was generated by imprecise *P*-element excision, which resulted in partial deletion of the *DmGSTO1* gene (Figure 5 and 6A). The $DmGSTO1^{null}$ mutant was viable and fertile, and it exhibited no obvious defects in adult morphology. In the *DmGSTO1* null mutant fly, there were no detectable levels of either *DmGSTO1A* or *DmGSTO1B* transcripts (Figure 6B). To determine expression pattern of DmGSTO1 during developmental stages, we performed qRT-PCR.

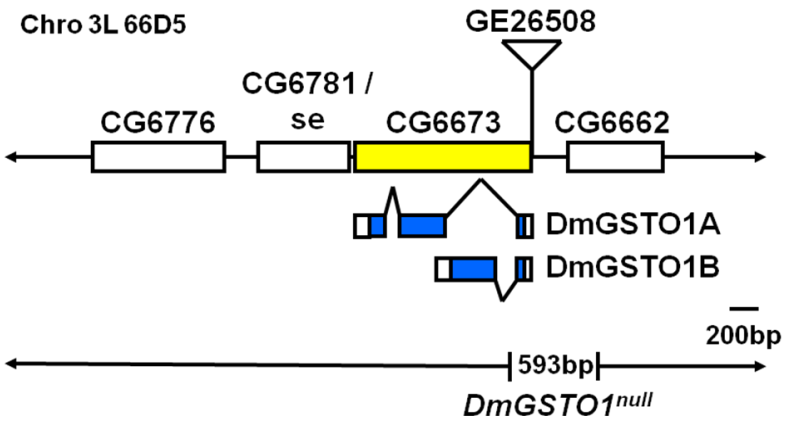

Figure 5. Genomic organization of the *DmGSTO1* locus

Genomic structures of D*mGSTO1* (*CG6673*). Transposon insertion sites are indicated above the map by an inverted triangle. The *GE26508 P*-element was imprecisely excised to generated $DmGSTO1^{null}$. $DmGSTO1^{null}$ was a 593 bp deletion, which removed the *DmGSTO1*, and *CG6662* coding regions. DmGSTO1 codes for two transcripts, A and B, which share the first exon.

Figure 6. Validation of *DmGSTO1* null mutant line

(A) Excision lines were molecularly characterized by genomic PCR. Expected band of wild-type shows 4.1 kb whereas excision lines show wild-type as well as deleted band. The break points of the deletion were determined by DNA sequencing. (B) Quantitative RT-PCR analysis on extracts from mutant and control flies. *DmGSTO1*^{null} mutants showed loss of the two transcripts (*DmGSTO1A* and *DmGSTO1B*), and *CG6662*. *GAPDH* was used as a control. *DmGSTO1*^{null} mutant do not affect other GSTO genes, *CG6781* (*sepia*) and *CG6776*. (C) Quantitative RT-PCR analysis of *DmGSTO1* expression during development. *rp49* was used as a control. The two transcripts of *DmGSTO1* can be detected during all developmental stages.

A

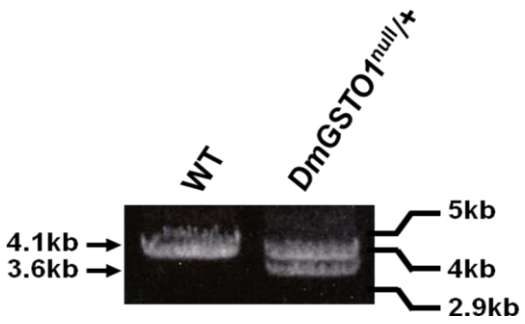
WT
DmGSTO1null/+
4.1kb
3.6kb
5kb
4kb
2.9kb

B

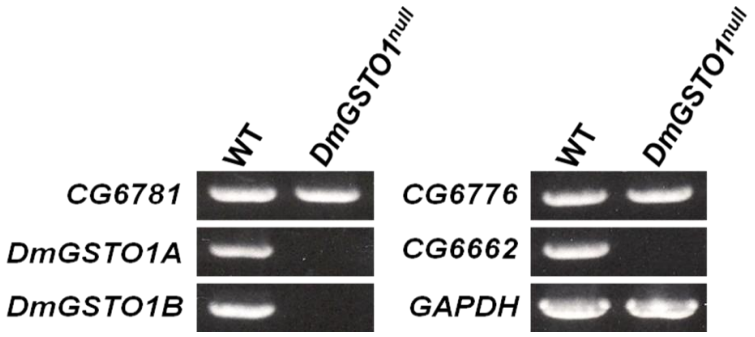
WT
DmGSTO1null
WT
DmGSTO1null
CG6781
DmGSTO1A
DmGSTO1B
CG6776
CG6662
GAPDH

C

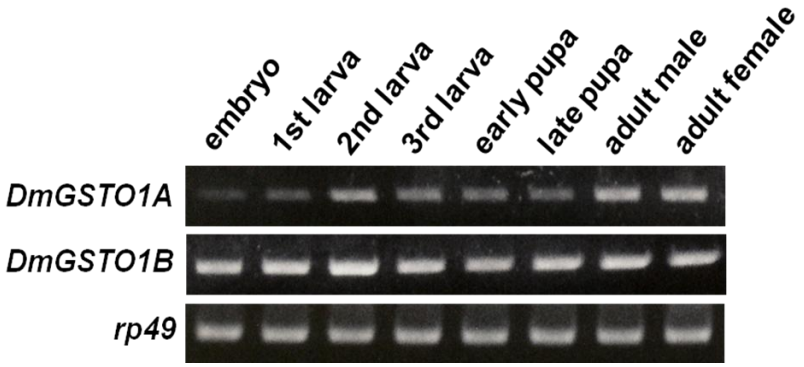
embryo
1st larva
2nd larva
3rd larva
early pupa
late pupa
adult male
adult female
DmGSTO1A
DmGSTO1B
rp49

DmGSTO1A and *DmGSTO1B* mRNAs were detected at all developmental stages (Figure 6C). GSTO enzymes exhibit higher glutathione-dependent thiol transferase and dehydroascorbate reductase (DHAR) activity than any other class of GSTs (Board *et al.*, 2000). We have shown that DmGSTO1B has much higher DHAR activity than DmGSTO1A *in vitro* (Kim *et al.*, 2006). The DHAR activity in *DmGSTO1*^{null} flies was dramatically decreased to ~5% of the DHAR activity found in wild-type flies (Figure 7). Furthermore, *DmGSTO1*^{null} mutants were sensitive to paraquat, an oxidative stress inducer (Figure 8). Using a ubiquitous driver, *Tub-Gal4*, we directed expression of DmGSTO1A or DmGSTO1B in the *DmGSTO1*^{null} mutant background. The paraquat sensitivity was rescued by expression of DmGSTO1B, which exhibited more oxidative stress protection than DmGSTO1A (Figure 8). These results suggest that the paraquat-sensitive phenotype in the *DmGSTO1*^{null} mutant is primarily due to the loss of DmGSTO1B function. Because DHAR catalyzes the conversion of dehydroascorbate (DHA) to ascorbate (AsA) using glutathione as a reducing agent, we investigated the level of DHA and AsA in the mutant flies. The level of AsA in fly extracts was detected by HPLC (Figure 9A, arrow; peak time, 4.7 min). As shown in Figure 9B, only the overexpression of DmGSTO1B rescued the AsA/DHA ratio in *DmGSTO1*^{null} mutants. These results indicate that DmGSTO1B has a protective role in response to paraquat-induced stress and plays an important role in the *in vivo* conversion of DHA to AsA.

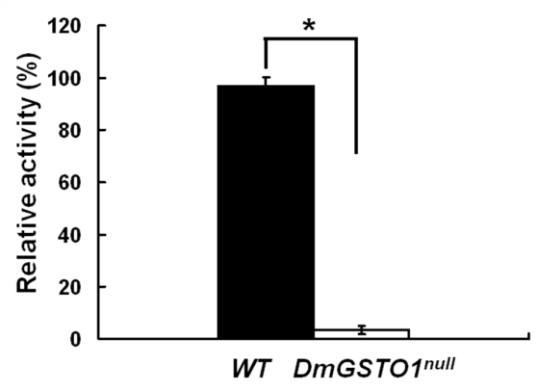

Figure 7. GSH-dependent DHA reductase assay

GSH-dependent DHA reductase activity in wild-type and *DmGSTO1*^{null}. *Error bars* indicate the standard deviation (S.D.). The experimental significance was determined by one-way ANOVA (*, $P < 0.0001$). Experiments were performed in triplicate.

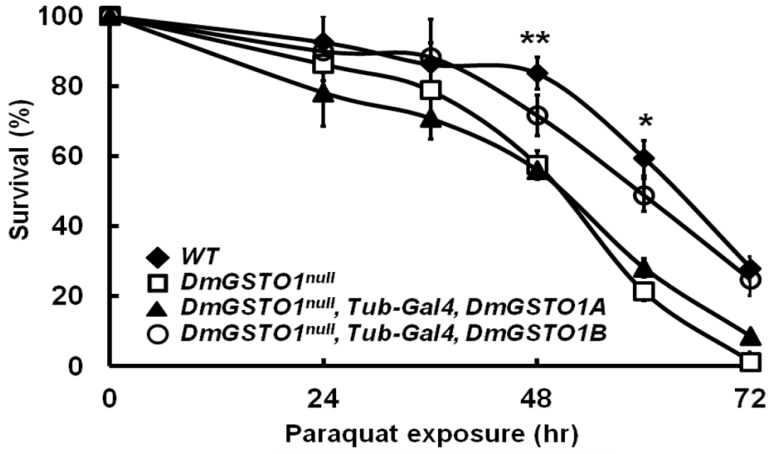

Figure 8. Sensitivity of DmGSTO1 mutants to oxidative stress

Survival rates of paraquat-treated (20 mM) flies overexpressing DmGSTO1A, and DmGSTO1B under the control of *Tubulin-Gal4*, a ubiquitously expressed driver ($n \geq 80$). *DmGSTO1*^{null} mutants were sensitive to oxidative stress. Overexpression of DmGSTO1B in a *DmGSTO1*^{null} mutant background reduced sensitivity to treatment with paraquat. *Error bars* indicate the standard deviation (S.D.). The significance was determined by one-way ANOVA (**, $P < 0.05$; *, $P < 0.01$).

Figure 9. Ascorbic acid and dehydroascorbic acid contents

(A) Chromatogram of ascorbic acid in fly extracts (solid line, arrow) and ascorbic acid specific-oxidase treated fly extracts (dash line). Samples were prepared as described in materials and methods. (B) Ascorbic acid and dehydroascorbic acid content in fly extracts. The level of AsA was lower in *DmGSTO1*^{null} flies than in wild-type flies, whereas DHA was higher in *DmGSTO1*^{null} flies than in wild-type flies. The AsA/DHA ratio decreased from 7.29 in wild-type to 3.28 in *DmGSTO1*^{null}. Overexpression of DmGSTO1B in a *DmGSTO1*^{null} mutant background restored the ratio of AsA/DHA to 6.35. *Error bars* indicate the standard deviation (S.D.). Experimental significance was determined by one-way ANOVA (**, $P < 0.01$; *, $P < 0.05$). Experiments were performed in triplicate.

A

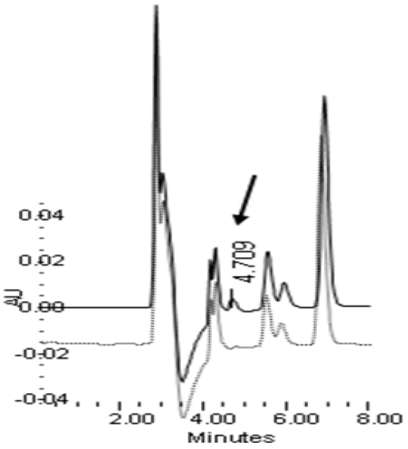
0.04
0.02
0.00
-0.02
-0.04
AU
4.709
2.00
4.00
6.00
8.00
Minutes

B

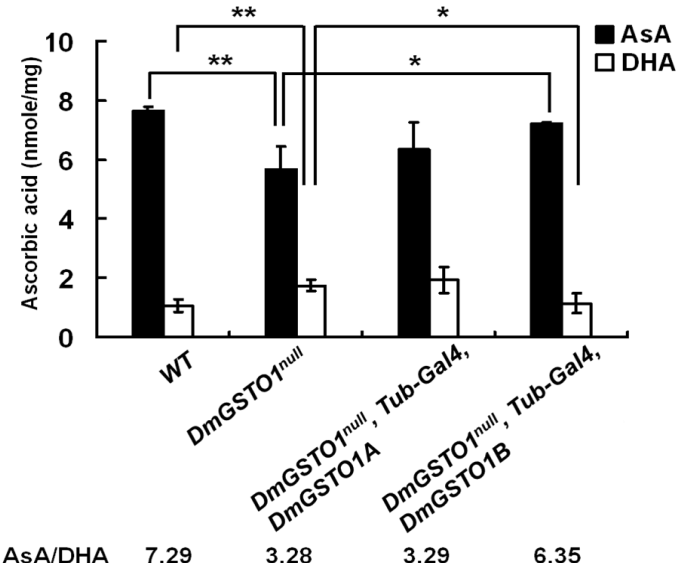
**
*
**
*
AsA
DHA
Ascorbic acid (nmole/mg)
10
8
6
4
2
0
WT
DmGSTO1null
DmGSTO1null, Tub-Gal4, DmGSTO1A
DmGSTO1null, Tub-Gal4, DmGSTO1B
AsA/DHA 7.29 3.28 3.29 6.35

2. DmGSTO1 partially rescues *park*^{1} mutant phenotypes.

Although it has been reported that GSTs are involved in neurodegenerative disease (Trinh *et al.*, 2008; Stroombergen and Waring, 1999; Smeyne *et al.*, 2007), the molecular function of GSTOs remains unknown. To investigate the biological function of DmGSTO1 in PD, we conducted genetic studies with *park*^{1} mutants. As reported previously (Cha *et al.*, 2005; Park *et al.*, 2006), *park*^{1} mutants showed collapsed thorax and downturned wing phenotypes. Surprisingly, increasing DmGSTO1A expression using the muscle-specific *24B-Gal4* driver significantly suppressed both thorax and wing phenotypes in *park*^{1} mutants, whereas increased DmGSTO1B expression showed no effects (Figure 10C, D, H, I and Figure 11A). Of the *GSTO* genes, only the transcriptional expression of *DmGSTO1*, (*CG6673*) was decreased in *park*^{1} mutants (Figure 12A). Because the level of *DmGSTO1* mRNA decreased in *park*^{1} mutants, we investigated whether the protein levels were also decreased in *park*^{1} mutants. We generated a specific antibody against DmGSTO1A. As shown in Figure 12B, the DmGSTO1A protein level was dramatically decreased in *park*^{1} mutants compared with wild-type flies. These results indicate that parkin regulates transcriptional expression of the *DmGSTO1* gene. We further examined the genetic interactions between parkin and DmGSTO1 by introducing a *DmGSTO1* null mutation in the *park*^{1} mutants. We found that the loss-of-function of *DmGSTO1* further enhanced the downturned wing and collapsed thorax phenotypes in the one-day-old *park*^{1} mutants (Figure 10K and Figure 11B). In the *DmGSTO1*^{null} mutant, neither *DmGSTO1* nor *CG6662* transcripts were detected (Figure 6B).

Figure 10. The defective thorax and downturned wing phenotypes

(A-L) Up-regulation of DmGSTO1A suppressed the collapsed thorax (white arrows) and downturned wing phenotypes of *parkin* mutant flies.

Figure 11. Up-regulation of DmGSTO1 suppresses the defective thorax and downturned wing phenotypes of *park*^{1} mutants.

(A) Statistically analysis of the percentage of collapsed thorax (n > 120) and downturned wing (n > 90) phenotypes in 3-day-old flies. DmGSTO1A overexpression by the *24B-Gal4* muscle-specific driver suppresses the thorax and wing defects of *parkin* mutant flies. *Error bars* indicate the standard deviation (S.D.). Experimental significance was determined by one-way ANOVA (**, $p < 0.005$; ns, not significant). (B) Percentage of collapsed thorax and downturned wing phenotypes in 1-day-old *park*^{1}*/DmGSTO1*^{null} double mutants. The *DmGSTO1* mutation enhanced the thorax and wing defects exhibited by *parkin* mutants. *Error bars* indicate the standard deviation (S.D.). Statistical analysis was carried out with one-way ANOVA (**, $P < 0.001$; *, $P < 0.05$).

A

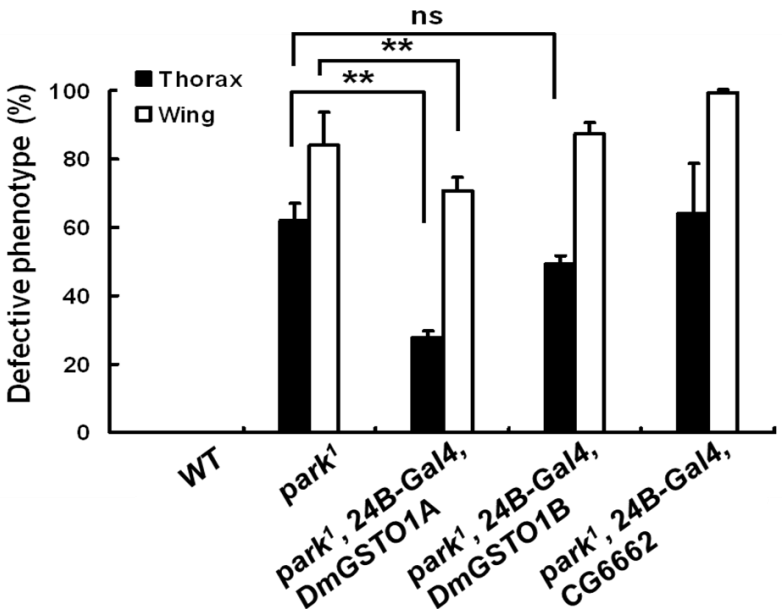
ns
**
**
Thorax
Wing
Defective phenotype (%)
100
80
60
40
20
0
WT
park1
park1, 24B-Gal4, DmGSTO1A
park1, 24B-Gal4, DmGSTO1B
park1, 24B-Gal4, CG6662

B

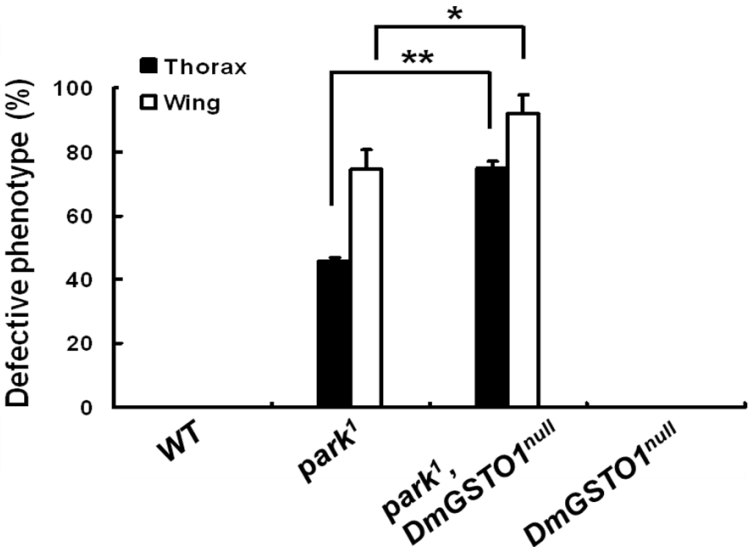
*
**
Thorax
Wing
Defective phenotype (%)
100
80
60
40
20
0
WT
park1
park1, DmGSTO1null
DmGSTO1null

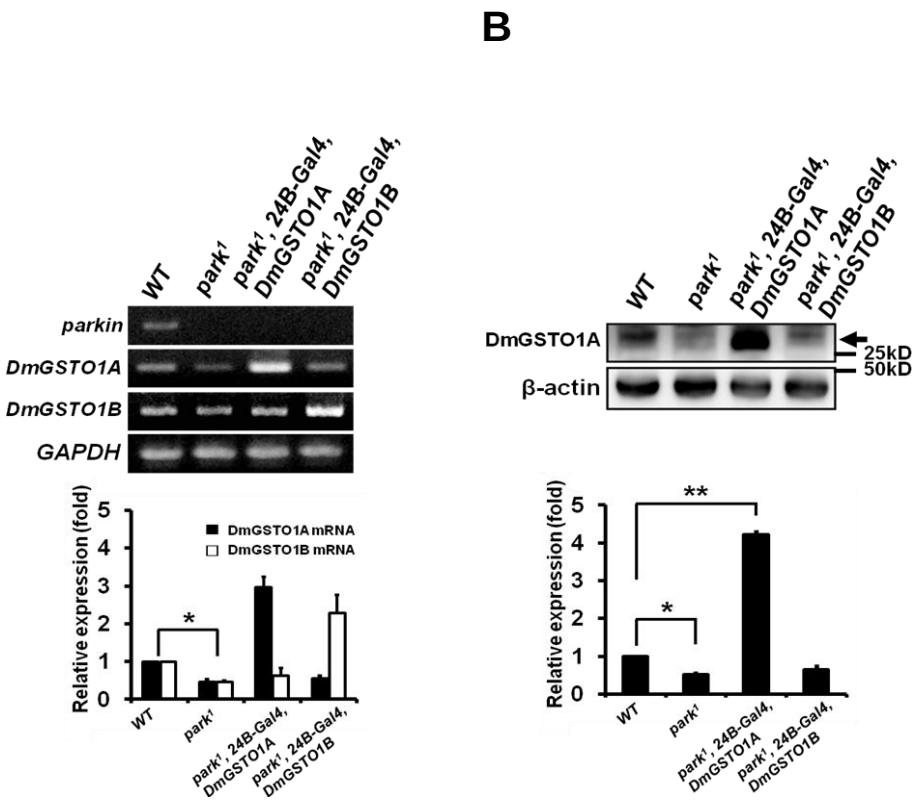

Figure 12. Expression levels of DmGSTO1 in *park*^{1} mutants

(A) DmGSTO1 mRNA levels determined by RT-PCR were also reduced in *park*^{1} mutants. *GAPDH* was used as a loading control. *Error bars* indicate the standard deviation (S.D.). Significance was determined by one-way ANOVA (*, $p < 0.01$). Experiments were performed in triplicate. (B) Western blot analysis of fly thorax extracts probed with anti-DmGSTO1A antibody. Endogenous DmGSTO1A levels (black arrow) were dramatically reduced in *park*^{1} mutants. β-actin was used as a loading control. *Error bars* indicate the standard deviation (S.D.). The significance was determined by one-way ANOVA (**, $P < 0.0001$; *, $P < 0.01$).

We could eliminate the possibility that CG6662 played a role in suppressing the *park*^{1} mutant phenotype by demonstrating that CG6662 overexpression in *park*^{1} mutants had no effect on the *park*^{1} mutant phenotype (Figure 10E, J and Figure 11A). These results indicate that CG6662 is not involved in the suppression of *parkin* mutant phenotypes. The downturned wing and thorax disruption phenotypes of *parkin* mutant flies are caused by the degeneration of the IFMs (Pesah *et al.*, 2004; Greene *et al.*, 2003). Therefore, we investigated whether DmGSTO1 prevented muscle degeneration in *park*^{1} mutants. As determined by histological analysis of thoracic IFMs, the integrity of IFMs in dorsal longitudinal muscles, which regulate adult wing posture, was clearly disrupted in *park*^{1} mutants (Figure 13A and B, red arrows; magnified view, Figure 13A' and B'). Although *DmGSTO1*^{null} mutants showed a normal muscle phenotype, *park*^{1}/*DmGSTO1*^{null} double mutants showed dramatically enhanced degeneration of IFMs compared with *park*^{1} single mutants (Figure 13B, D, B', and D'). Furthermore, overexpression of DmGSTO1A using a ubiquitous driver, *Tub-Gal4*, suppressed the degeneration of IFMs in *park*^{1} mutants. Overexpression of DmGSTO1A in *park*^{1} mutants resulted in regular and compact muscle tissues in the dorsal longitudinal IFMs, which were similar to those of wild-type flies except for occasional vacuoles (Figure 13C and C'). These data suggest that DmGSTO1 expression partially rescues the morphological defects and muscle degeneration in *park*^{1} mutants.

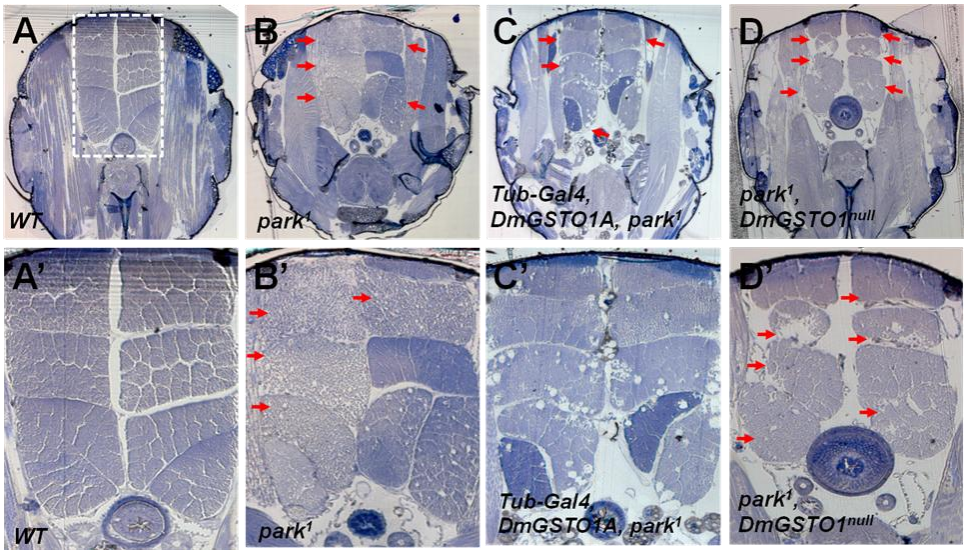

Figure 13. DmGSTO1 expression partially rescues the muscle degeneration in *park*^{1} mutants.

(A-D) Light microscopy was used to examine IFM morphology (red arrows, muscle degeneration). Shown are magnified views of the dorsal longitudinal muscle (X 200, A'-D'). *Tubulin-Gal4*-driven DmGSTO1A expression rescues muscle degeneration of *park*^{1} mutants flies. The *park*^{1}/*DmGSTO1*^{null} double mutants showed enhanced degeneration of muscles compared with *park*^{1} single mutants.

3. phospho-JNK signal and apoptosis are suppressed by DmGSTO1 in *park*^{1} mutants.

Many studies have suggested that neuronal cell death in various neurodegenerative diseases is closely related to JNK activation. Cha *et al* (Cha *et al.*, 2005) reported that parkin inhibits the JNK pathway. As shown in Figure 14, phospho-JNK was dramatically increased in IFMs of the *park*^{1} mutant, whereas there was no change in phospho-JNK in the *DmGSTO1*^{null} mutant compared with wild-type. The expression of DmGSTO1A suppressed activation of phospho-JNK in *park*^{1} mutants (Figure 14A, B, and D), and the degree of suppression was confirmed by Western blot analysis (Figure 14E). Degeneration of IFMs in *parkin* mutants occurs through an apoptotic mechanism (Greene *et al.*, 2003). The IFMs in *park*^{1} mutants were examined by a terminal deoxynucleotidyltransferase-mediated dUTP end labeling (TUNEL) assay. As shown in Figure 15, the increased TUNEL signal in *park*^{1} mutants was suppressed by DmGSTO1A expression, similar to the suppression in the phospho-JNK signal. These data suggest that DmGSTO1 prevents degeneration of IFMs by blocking the activation of JNK and apoptosis in *park*^{1} mutants.

Figure 14. phospho-JNK signal is suppressed by DmGSTO1 in *park*^{1} mutants.

(A) Muscle-specific expression of DmGSTO1A in *park*^{1} mutants reduced phosphorylated JNK. Activated JNK (phospho-JNK; p-JNK) is visualized in green, and phalloidin-labeled muscle tissues are shown in red. (B) Western blot analysis of phospho-JNK. *Error bars* indicate the standard deviation (S.D.). Experimental significance was determined by one-way ANOVA (*, $p < 0.05$). Experiments were performed in triplicate.

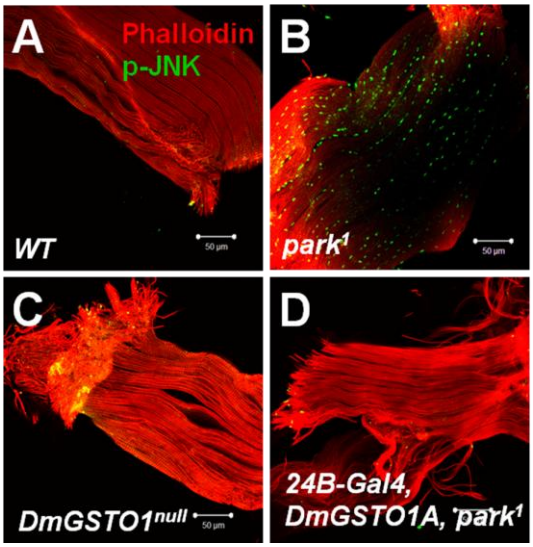
A
Phalloidin
p-JNK
WT
B
park1
C
DmGSTO1null
D
24B-Gal4,
DmGSTO1A, park1

E

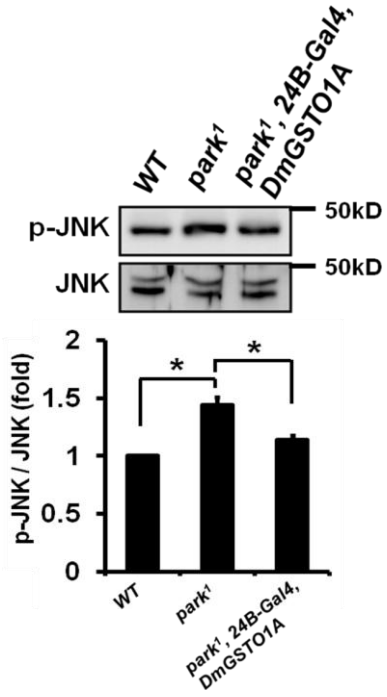
WT
park1
park1, 24B-Gal4,
DmGSTO1A
p-JNK
50kD
JNK
50kD
p-JNK / JNK (fold)
2
1.5
1
0.5
0
*
*
WT
park1
park1, 24B-Gal4,
DmGSTO1A

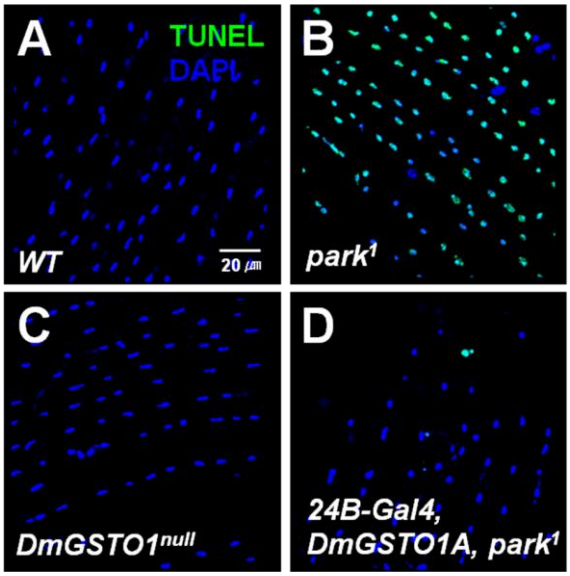

Figure 15. Apoptotic cell death caused by loss of *pakin* is rescued by DmGSTO1 overexpression in the muscle.

(A-D) TUNEL assay in thorax muscle. Merged images of apoptotic cells (TUNEL, green) and nuclei (DAPI, blue). Up-regulation of DmGSTO1A resulted in fewer apoptotic cells in the muscle.

4. DmGSTO1 suppresses dopaminergic neuronal degeneration in *park*^{1} mutants.

park^{1} mutants show an age-dependent degeneration of DA neurons, especially in the protocerebral posterior lateral 1 (PPL1) cluster (Cha *et al.*, 2005; Wang *et al.*, 2007). To further clarify the effect of DmGSTO1on *park*^{1} mutants, we examined the degeneration of DA neurons that is characteristic of PD. As shown in Figure 16, DmGSTO1A expression under the control of a DA neuron-specific tyrosine hydroxylase (*TH*)-*Gal4* driver resulted in significant restoration of the lost DA neurons in 20-day-old *park*^{1} mutant flies. In addition, 20-day-old *park*^{1}/*DmGSTO1*^{null} double mutants showed significantly increased DA neuron degeneration in the PPL1 cluster compared with the *park*^{1} single mutants of the same age, whereas there was no difference in neuronal degeneration between *park*^{1}/*DmGSTO1*^{null} double mutants and *park*^{1} single mutants in 1-day-old flies (Figure 17). These results indicate that DmGSTO1 protects the DA neurons from age-dependent degeneration in *park*^{1} mutants.

Figure 16. Overexpression of DmGSTO1 can suppress degeneration of dopaminergic neurons in *park*^{1} mutants.

(A-D) Whole-mount adult male brains (20-day-old) showing dopaminergic neuron clusters, PPL1 marked by anti-TH antibody (red). (E) Quantification of TH-positive neurons in PPL1 clusters in 20-dya-old flies (n > 10). Up-regulation of DmGSTO1A by the *TH-Gal4*, dopaminergic neuron-specific driver can rescue dopaminergic neuron loss in *park*^{1} mutants. *Error bars* indicate the standard deviation (S.D.). Experimental significance was determined by one-way ANOVA (***, $p < 0.0001$).

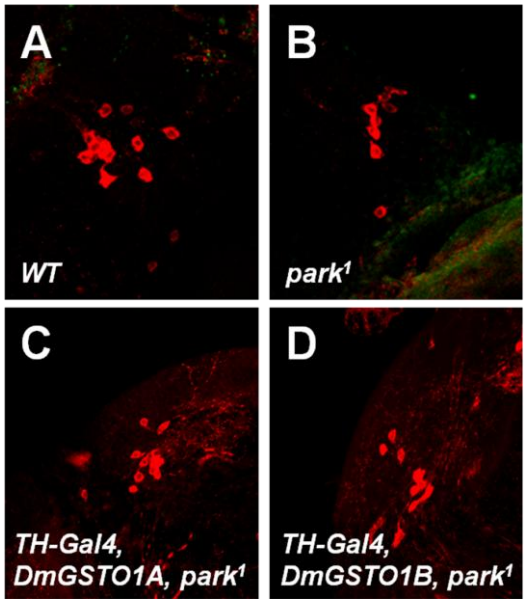
A
WT
B
park1
C
TH-Gal4,
DmGSTO1A, park1
D
TH-Gal4,
DmGSTO1B, park1

E

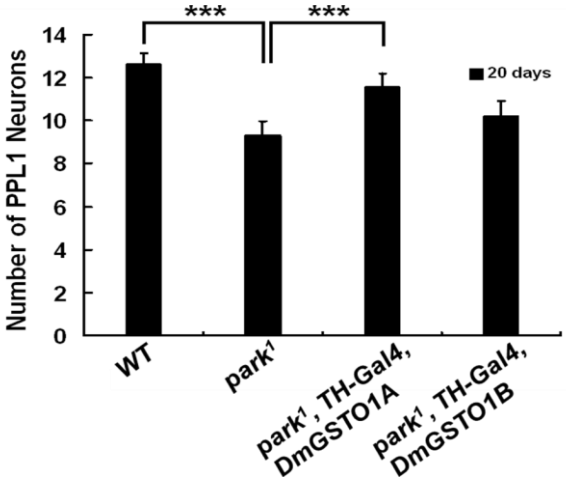
***
***
20 days
Number of PPL1 Neurons
0
2
4
6
8
10
12
14
WT
park1
park1, TH-Gal4,
DmGSTO1A
park1, TH-Gal4,
DmGSTO1B

Figure 17. Degeneration of dopaminergic neuron induced by loss of *parkin* is enhanced by *DmGSTO1* mutation.

(A-G) Representative image from adult brains immunostained with anti-TH antibody to mark dopaminergic neurons. (H) Quantification of TH-positive neurons in PPL1 clusters in 1- and 20-day-old flies (n > 10). 20-day-old $park^{1}/DmGSTO1^{null}$ double mutants showed significantly increased dopanminergic neuron degeneration in the PPL1 cluster compared with $park^{1}$ single mutants. *Error bars* indicate the standard deviation (S.D.). Experimental significance was determined by one-way ANOVA (***, $p < 0.0001$).

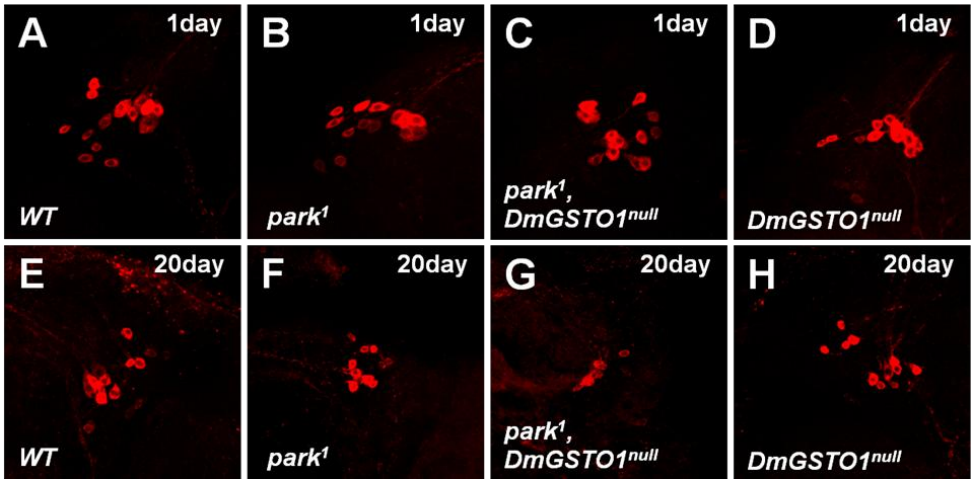
A
1day
WT
B
1day
park1
C
1day
park1,
DmGSTO1null
D
1day
DmGSTO1null
E
20day
WT
F
20day
park1
G
20day
park1,
DmGSTO1null
H
20day
DmGSTO1null

I

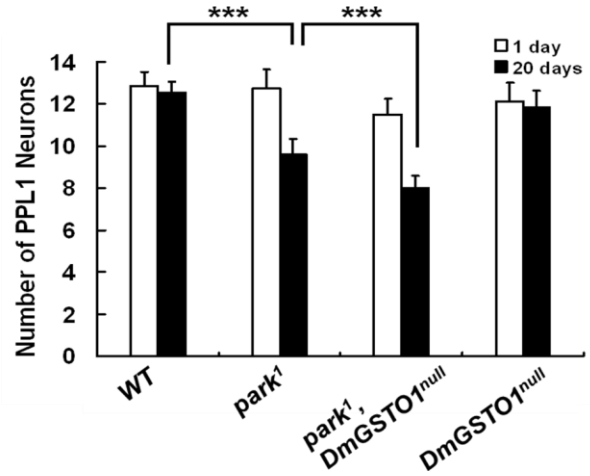
***
***
1 day
20 days
Number of PPL1 Neurons
0
2
4
6
8
10
12
14
WT
park1
park1,
DmGSTO1null
DmGSTO1null

5. DmGSTO1 restores accumulation of tubulin in IFMs in *park*^{1} mutants.

Parkin functions as an E3 ubiquitin ligase and has important roles in the degradation of many substrates (Zhang *et al.*, 2000; Shimura *et al.*, 2000). Recent *in vitro* studies demonstrated that parkin binds to microtubule and tubulin proteins with high affinity and that parkin ubiquitinates and promotes the degradation of α/β-tubulin (Ren *et al.*, 2003). It remains controversial whether putative *in vitro* substrates are relevant *in vivo*. Therefore, we investigated the α/β-tubulin protein levels in *park*^{1} mutants *in vivo*. Levels of α-tubulin were increased in *park*^{1} mutant muscles (Figure 18A and B). Interestingly, the accumulation of α-tubulin in *park*^{1} mutant muscles was dramatically reduced by DmGSTO1A expression, and it was enhanced in *park*^{1}/*DmGSTO1*^{null} double mutant muscles (Figure 18B, C and D). The levels of actin filaments in IFMs were unchanged in all mutants (Figure 18F-J). These changes were confirmed by Western blot analysis (Figure 19A and B).We found that tubulin was slightly increased in *DmGSTO1*^{null} mutants by Western blot analysis (Figure 19B). We also detected tubulin accumulation in DA neurons in *park*^{1} mutants and *park*^{1}/*DmGSTO1*^{null} double mutants (Figure 20, white arrowheads). These data indicate that parkin does not directly regulate the level of tubulin in *Drosophila in vivo*. In contrast to the change in total protein levels (Figure 19A), there were no detectable changes in the α/β-*tubulin* transcript levels in *park*^{1} mutants regardless of DmGSTO1A expression level (Figure 21). Thus, the increased α/β-tubulin levels were not caused by increased transcription but by protein accumulation. These results indicate that parkin is required for the regulation of tubulin levels and that DmGSTO1 suppresses the accumulation of tubulin in *park*^{1} mutants.

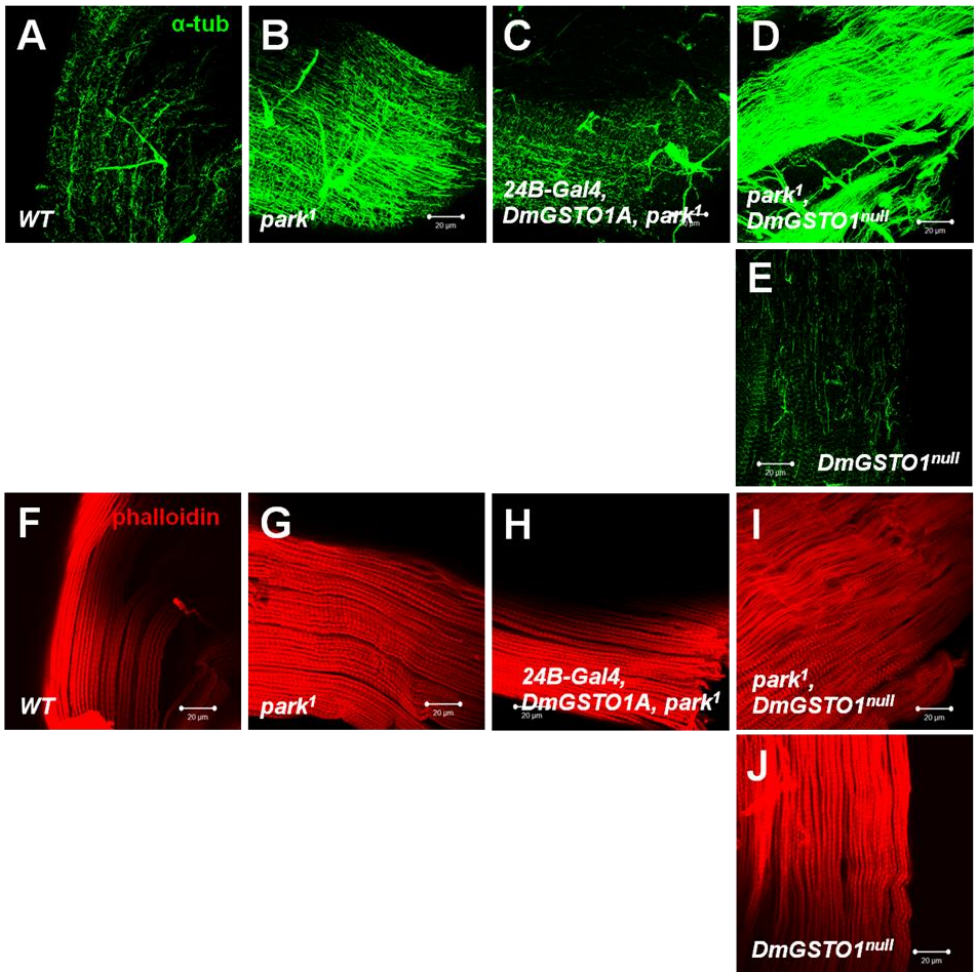

Figure 18. The accumulation of tubulin in *park*^{1} mutant muscle tissues was dramatically reduced by DmGSTO1 expression.

(A-J) Shown are representative images of flight muscle stained with anti-α-tubulin antibody and phalloidin. α-tubulin accumulates in *park*^{1} mutant muscle. The accumulation of tubulin in the *park*^{1} mutant was suppressed by the muscle-specific up-regulation of DmGSTO1A. The levels of actin filaments in muscle did not change in any mutants as visualized with phalloidin. The scale bar represents 20 μm.

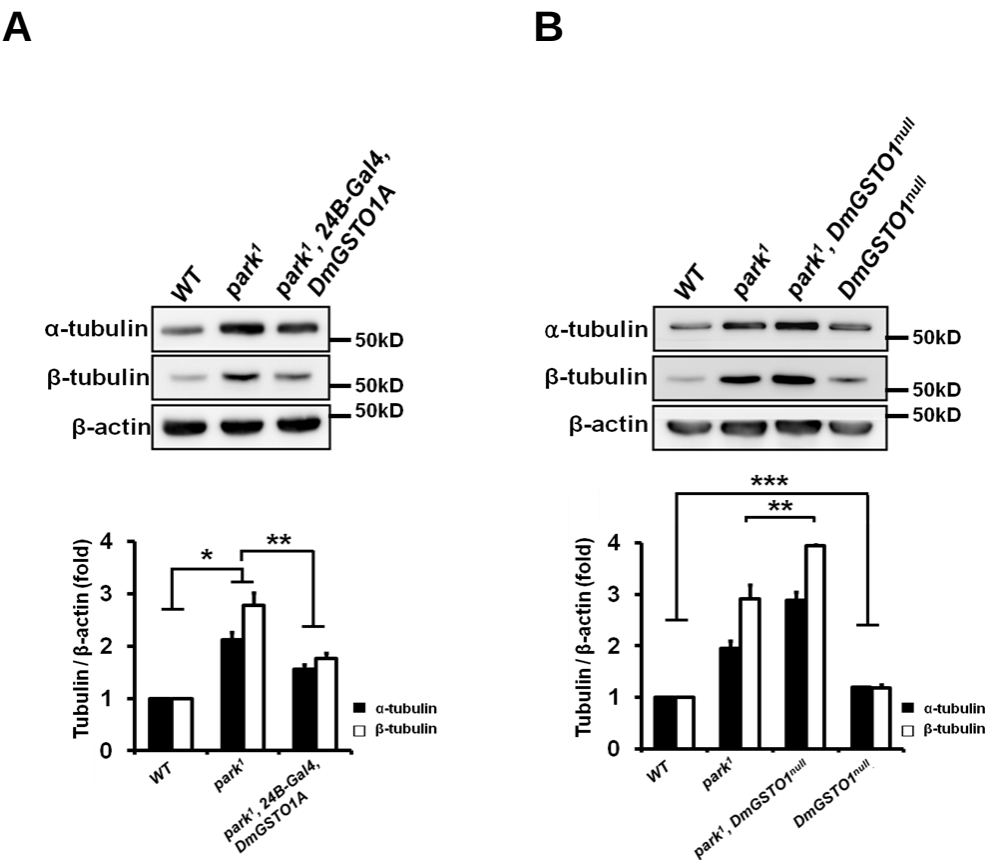

Figure 19. Expression of DmGSTO1 affects the protein levels of tubulin in *park*^{1} mutant.

Western blots with anti-α-tubulin and anti-β-tubulin antibodies. β-actin was used as a loading control. (A) The increased levels of α/β-tubulin in *park*^{1} mutants were rescued by DmGSTO1A expression. *Error bars* indicate the standard deviation (S.D.). The experimental significance was determined by one-way ANOVA (**, $p < 0.05$; *, $p < 0.001$). (B) Tubulin levels were higher in the double mutants than in the *park*^{1} single mutants. *Error bars* indicate the standard deviation (S.D.). The significance was determined by one-way ANOVA (***, $p < 0.01$; **, $p < 0.001$).

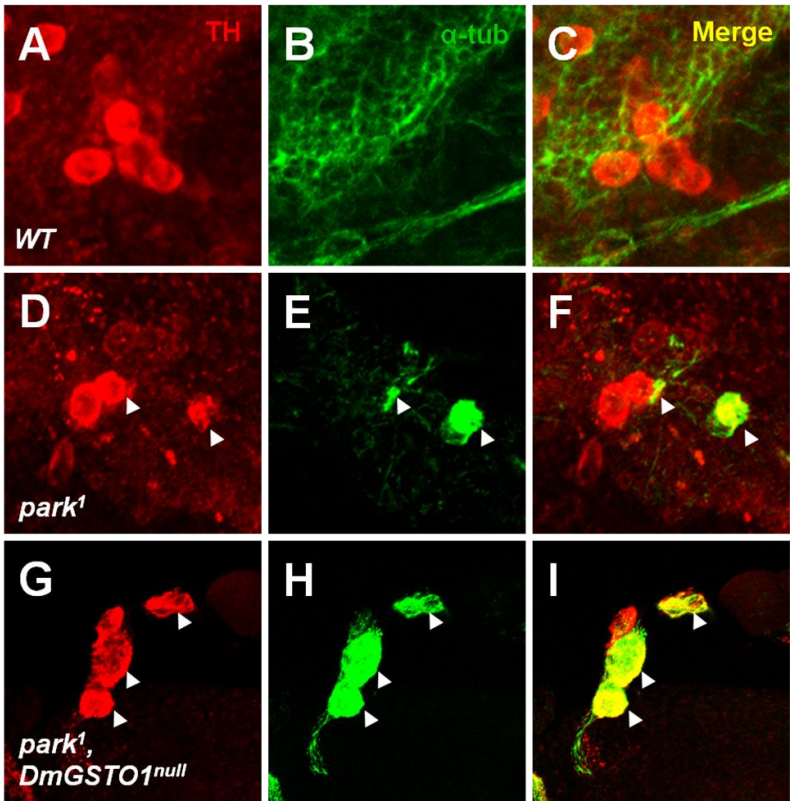

Figure 20. *park*^{1} mutants display accumulation of tubulin in dopaminergic neurons.

(A-I) Immunostaining with anti-α-tubulin and anti-TH antibodies in dopaminergic neurons in *Drosophila* brains. (D-I) Accumulation of α-tubulin was observed in dopaminergic neurons from *park*^{1} mutants and *park*^{1}*/DmGSTO1*^{null} double mutants (white arrowheads). Immunostaining with anti-TH antibody was performed to identify dopaminergic neurons.

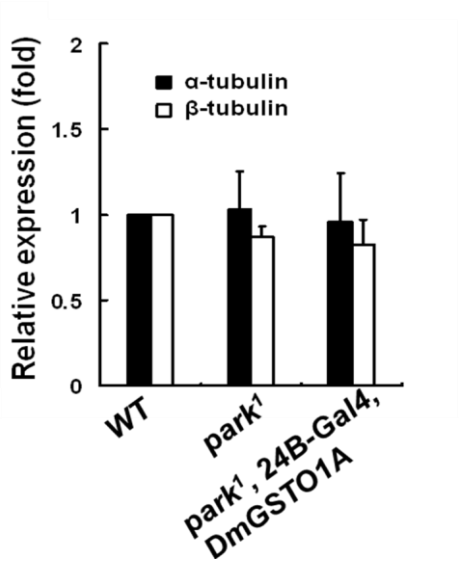

Figure 21. α/β-tubulin transcript levels in *park*^{1} mutants

mRNA levels of male thoraces were determined by real-time PCR analysis. Relative amounts of tubulin mRNA were unchanged in all mutants. *Error bars* indicate the standard deviation (S.D.).

6. DmGSTO1 suppresses activation of unfolded protein response (UPR) in *park*^{1} mutant muscles.

Many studies have claimed that ER stress is involved in the progression of neurodegenerative diseases, such as PD. The UPR is a signaling pathway that is activated in response to ER stress. UPR activation has been observed in DA neurons of PD patients and is exemplified by an increase in phospho-PERK and eIF2α (Hoozemans *et al.*, 2007). To determine whether the *parkin* mutation induces UPR activation, we examined eIF2α, which is one of the components of the UPR signaling pathway and is activated by the upstream kinase PERK (Smith *et al.*, 2005). The level of active phospho-eIF2α was highly increased in *park*^{1} mutants and dramatically restored by DmGSTO1A expression (Figure 22). The ER and mitochondrial UPR share similar pathways that increase chaperone levels to promote protein homeostasis in the cytoplasm and mitochondria (Haynes and Ron, 2010). We also examined heat shock proteins (HSPs), including Hsp60, and Hsp/Hsc70. As shown in Figure 23, the levels of HSPs were increased in *park*^{1} mutants and reduced by DmGSTO1A expression. These data indicate that DmGSTO1 suppresses UPR activation in *park*^{1} mutants.

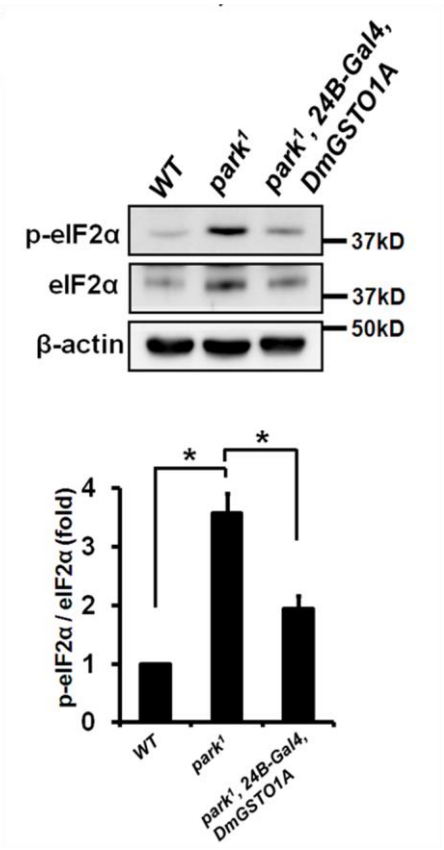

Figure 22. DmGSTO1 overexpression suppresses the increased level of phosphorylated eIF2α induced by *parkin* loss-of-function.

Western blot analysis of phosphorylated and total eIF2α. *Error bars* indicate the standard deviation (S.D.). The significance was determined by one-way ANOVA (*, $p < 0.05$). β-actin was used as a loading control. Experiments were performed in triplicate.

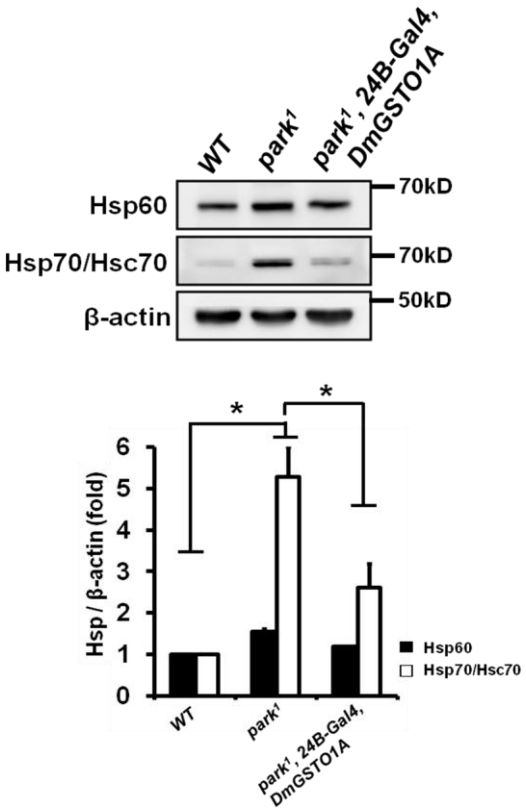

Figure 23. The levels of heat shock proteins were increased in *park*^{1} mutants and restored by up-regulation of DmGSTO1.

Western blot analysis of heat shock proteins (HSPs). Increased HSPs in *park*^{1} mutants were decreased with the up-regulation of DmGSTO1A. *Error bars* indicate the standard deviation (S.D.). The experimental significance was determined by one-way ANOVA (*, $p < 0.05$). β-actin was used as a loading control. Experiments were performed in triplicate.

7. DmGSTO1 restores mitochondrial ATP synthase activity in *park*^{1} mutants.

We next examined whether the catalytic activity of DmGSTO1A was critical for the rescue the *park*^{1} mutant phenotypes. GSTOs have a unique cysteine at their active site that binds to GSH (Board *et al.*, 2000). We constructed a catalytically inactive form of DmGSTO1A, DmGSTO1A^{C31A}, in which cysteine 31 was mutated to alanine (Figure 24A). In contrast to wild-type DmGSTO1A, expression of DmGSTO1A^{C31A} in muscle did not rescue the collapsed thorax and downturned wing phenotypes in *park*^{1} mutants (Figure 24B). Moreover, tubulin accumulation was not suppressed by DmGSTO1A^{C31A} expression in *park1* mutants (Figure 24C). Our data demonstrate that DmGSTO1 catalytic activity is required to rescue the defective phenotypes of *park*^{1} mutants.

Although the ability of DmGSTO1B to respond to oxidative stress was higher than that of DmGSTO1A, only up-regulation of DmGSTO1A suppressed the defective phenotypes in *parkin* mutants (Figure 8 and 11). Therefore, DmGSTO1A may suppress *parkin* mutant phenotypes by other mechanisms. The catalytic detoxification functions of the GST family have been studied by several research groups. However, some members of the GST family have physiological functions unrelated to detoxification (Tew and Townsend, 2011). Previous reports revealed that the rate of protein glutathionylation, a post-translational modification that regulates the function of proteins, is enhanced by the presence of active GSTP (GST Pi family) (Townsend *et al.*, 2009).

Figure 24. The catalytic activity of DmGSTO1 is critical for rescue of the defective phenotypes of the *park*^{1} mutant.

(A) Construction of a catalytically inactive form of DmGSTO1A, DmGSTO1^{C31A}, in which cysteine 31 was mutated to alanine at GSH binding site. (B) Expression of DmGSTO1A^{C31A} in the *park*^{1} mutant background did not suppress the collapsed thorax (n > 200) and downturned wing (n > 160) phenotypes of *parkin* mutants. *Error bars* indicate the standard deviation (S.D.). The experimental significance was determined by one-way ANOVA (*, $p < 0.05$). (C) Western blot analysis of adult thorax extracts using anti-β-tubulin antibodies. DmGSTO1A^{C31A} expressed in the *park*^{1} mutants did not rescue the tubulin accumulation phenotypes. *Error bars* indicate the standard deviation (S.D.). The significance was determined by one-way ANOVA (**, $p < 0.05$; *, $p < 0.01$). β-actin was used as a loading control. Experiments were performed in triplicate.

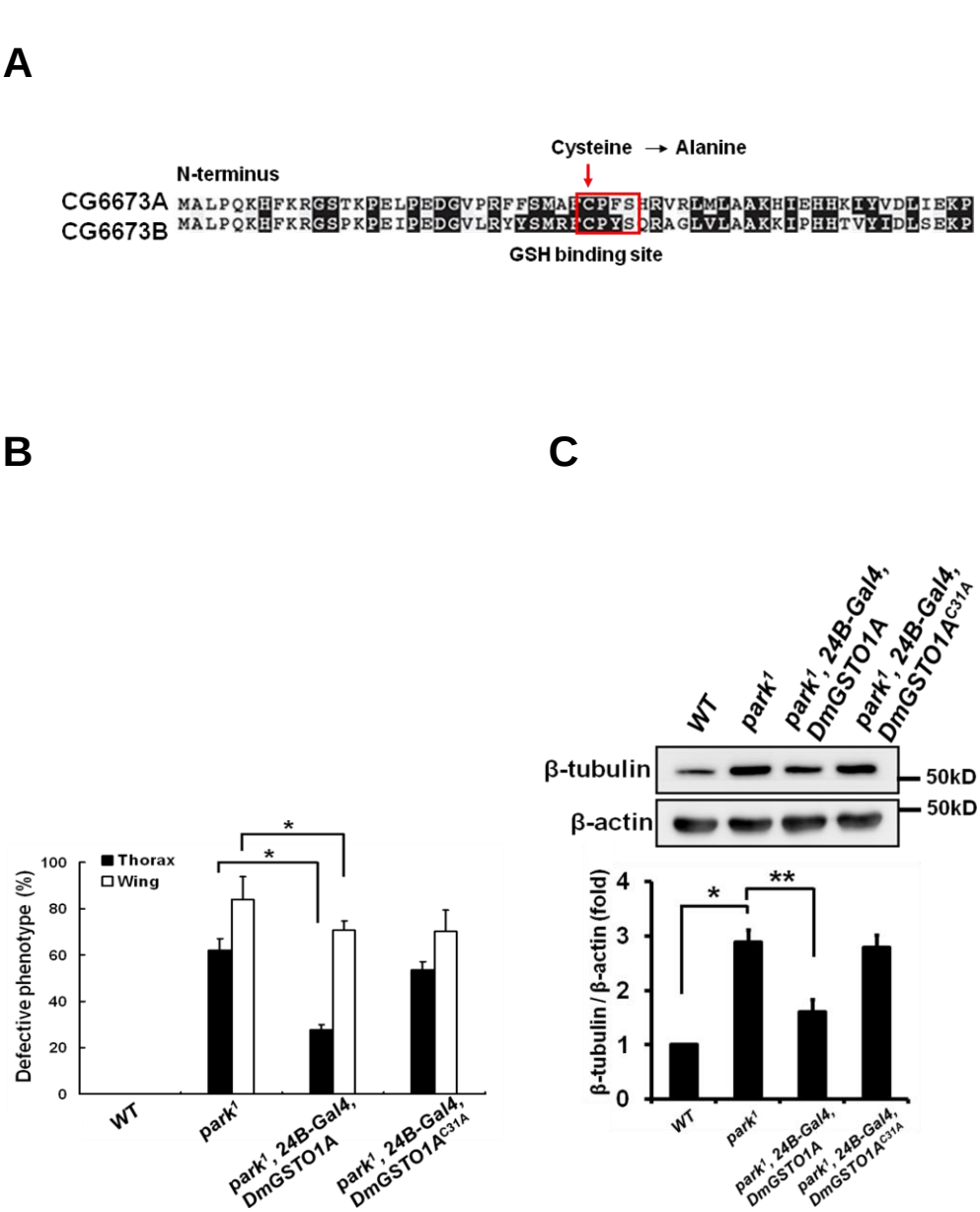
A
Cysteine → Alanine
N-terminus
CG6673A
CG6673B
GSH binding site
B
Thorax
Wing
Defective phenotype (%)
WT
park1
park1, 24B-Gal4, DmGSTO1A
park1, 24B-Gal4, DmGSTO1AC31A
C
β-tubulin
β-actin
50kD
50kD
β-tubulin / β-actin (fold)

Based on the result that DmGSTO1 enzyme activity is required to suppress the *parkin* mutant phenotypes, we screened *in vivo* targets of DmGSTO1 by immnunoprecipitation with an anti-GSH antibody in adult thorax extracts. Only one glutathionylated protein showed altered abundance in *park*^{1} mutants (Figure 25). DmGSTO1A expression increased the level of glutathionylation of this protein, whereas DmGSTO1A^{C31A} did not (Figure 25, arrow). The protein was identified by MALDI-TOF mass spectrometric analysis as the mitochondrial F_1F_0-ATP synthase β subunit. We also confirmed that DmGSTO1A can directly glutathionylate the ATP synthase β subunit in a dose-dependent manner in the presence of GSH (Figure 26). Furthermore, the endogenous levels of the glutathionylated form of the ATP synthase β subunit in thorax extracts were decreased in *park*^{1} mutants and decreased even more in *park*^{1}*/DmGSTO1*^{null} double mutants, whereas the total expression levels of the ATP synthase β subunit were unchanged in all fly lines. DmGSTO1A expression in *park*^{1} mutants restored the levels of glutathionylated ATP synthase β subunit to wild-type levels, whereas the expression of DmGSTO1A^{C31A} or DmGSTO1B in *park*^{1} mutants had no effect on the level of ATP synthase β subunit glutathionylation (Figure 27). However, in the *DmGSTO1*^{null} mutant, the level of glutathionylation of the ATP synthase β subunit was only slightly decreased compared with control. This finding suggests that a compensatory mechanism related to glutathionylation of the ATP synthase β subunit exists. Another DmGSTO, CG6662, did not affect glutathionylation of the ATP synthase β subunit (Figure 28).

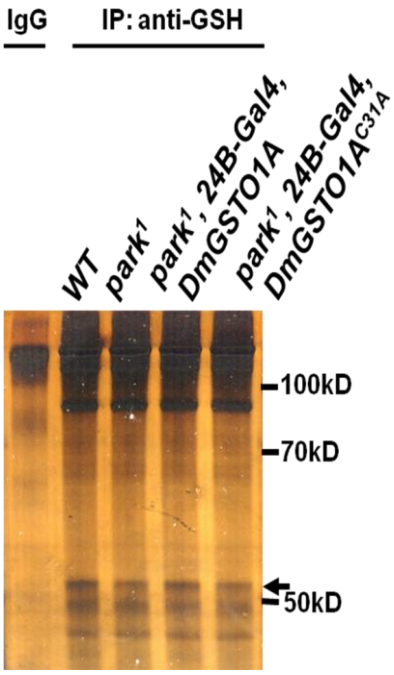

Figure 25. ATP synthase β subunit is a novel target of DmGSTO1.

Glutathionylated proteins were immunoprecipitated from thorax extracts of *park*^{1} mutants with an anti-GSH antibody. The products were separated by SDS-PAGE and then visualized by silver staining. Only one glutathionylated protein showed altered abundance in *park*^{1} mutants (arrow). Overexpression of DmGSTO1A increased the level of glutathionylation of this protein, whereas DmGSTO1A^{C31A} did not. The bands were manually excised from the gel and identified by MALDI-TOF mass spectrometric analysis.

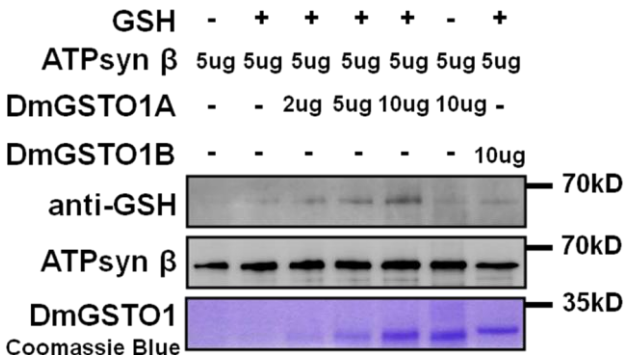

Figure 26. *in vitro*, glutathionylation of ATP synthase β subunit by DmGSTO1

In the presence of GSH, recombinant ATP synthase β subunit was glutathionylated by DmGSTO1A in a dose-dependent manner. However, ATP synthase β subunit was not glutathionylated by DmGSTO1B.

Figure 27. DmGSTO1 regulates glutathionylation of endogenous ATP synthase β subunit in *park*^{1} mutants.

Glutathionylated proteins were immunoprecipitated from thorax extracts with an anti-GSH antibody and were immnunoblotted with an anti-ATP synthase β antibody. Glutathionylation of endogenous ATP synthase β subunit in *park*^{1} mutants was regulated by the GSH-conjugating catalytic activity of DmGSTO1A but not by DmGSTO1B. The endogenous levels of the glutathionylated form of the ATP synthase β subunit were decreased even more in *park*^{1}*/DmGSTO1*^{null} double mutants. *Error bars* indicate the standard deviation (S.D.). The experimental significance was determined by one-way ANOVA (*, $p < 0.05$). β-actin was used as a loading control. Experiments were performed in triplicate.

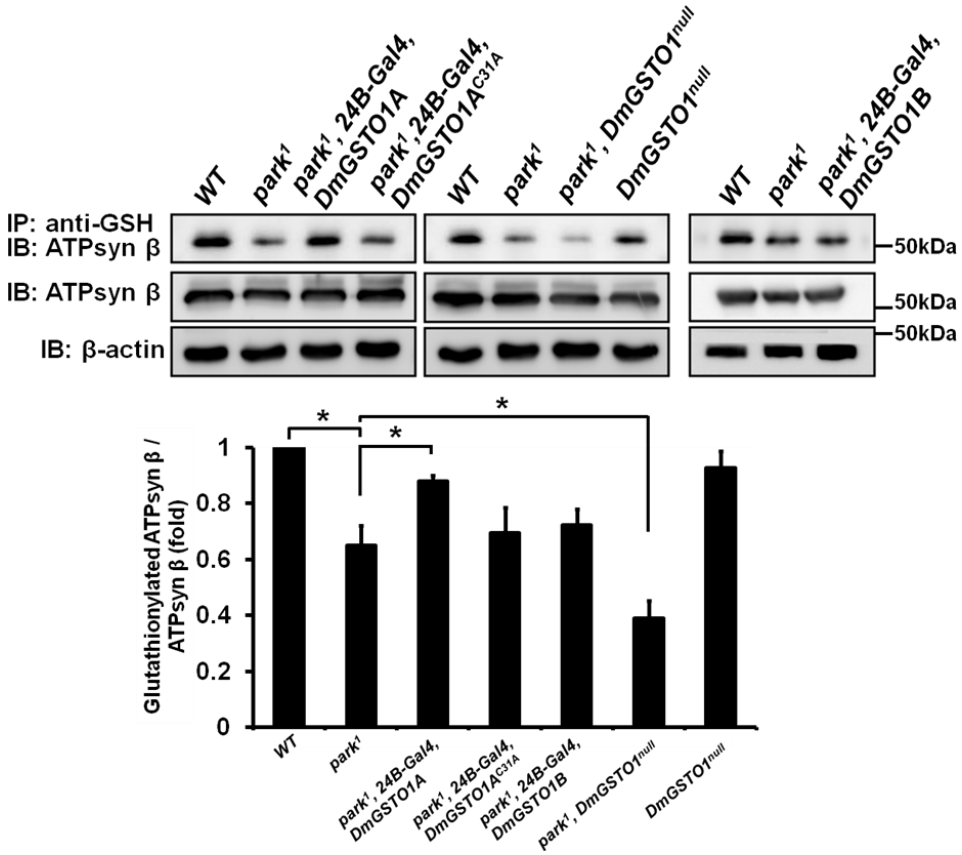
WT
park1
park1, 24B-Gal4, DmGSTO1A
park1, 24B-Gal4, DmGSTO1AC31A
WT
park1
park1, DmGSTO1null
DmGSTO1null
WT
park1
park1, 24B-Gal4, DmGSTO1B
IP: anti-GSH
IB: ATPsyn β
IB: ATPsyn β
IB: β-actin
50kDa
50kDa
50kDa
Glutathionylated ATPsyn β / ATPsyn β (fold)
0
0.2
0.4
0.6
0.8
1
*
*
*
WT
park1
park1, 24B-Gal4, DmGSTO1A
park1, 24B-Gal4, DmGSTO1AC31A
park1, 24B-Gal4, DmGSTO1B
park1, DmGSTO1null
DmGSTO1null

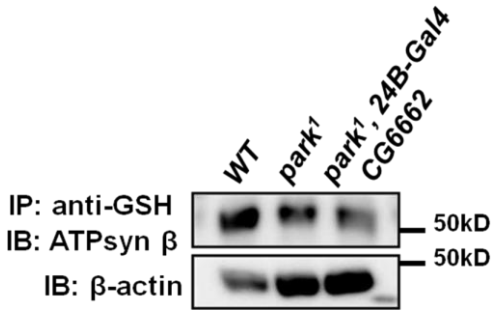

Figure 28. CG6662, another GSTO in *Drosophila*, was unable to rescue glutathionylation of the ATP synthase β subunit in *park*^{1} mutants.

Glutathionylated proteins were immunoprecipitated from thorax extracts with an anti-GSH antibody and were immnunoblotted with an anti-ATP synthase β antibody. CG6662 was unable to glutathionylate the endogenous ATP synthase β subunit in *park*^{1} mutants. β-actin was used as a loading control.

These data indicate that the ATP synthase β subunit is a novel and specific target of DmGSTO1A in *Drosophila* and that only DmGSTO1A expression in *park*^{1} mutants is sufficient to partially restore glutathionylation of the ATP synthase β subunit.

Glutathionylation is a reversible post-translational modification that can lead to alteration of protein or enzyme function, such as the Ca^{2+} uptake activity of the sarco-/endoplasmic reticulum calcium ATPase (Adachi *et al.*, 2004). To test the hypothesis that glutathionylation of the ATP synthase β subunit by DmGSTO1A in *park*^{1} mutants regulates ATP synthase activity, we isolated mitochondria from the thorax and measured F_1F_0-ATP synthase activity. As shown in Figure 29, the level of mitochondrial F_1F_0-ATP synthase activity was partially rescued by DmGSTO1Aexpression in *park*^{1} mutants and was decreased in *park*^{1}/*DmGSTO1*^{null} double mutants. Indeed, the change in mitochondrial F_1F_0-ATP synthase activity was correlated to the change in glutathionylation of the ATP synthase β subunit. Consistent with the ATP synthase activity results, we observed a change in the total ATP levels in all of the mutant lines (Figure 29). Impaired mitochondrial respiration caused by decreased ATP production has been reported in PD, and agents that improve mitochondrial respiration can exert beneficial effects in animal models of PD (Abou-Sleiman *et al.*, 2006). These reports are consistent with our findings; ATP synthase activity and ATP levels are significantly decreased in *park*^{1} mutants and can be modulated by DmGSTO1 expression.

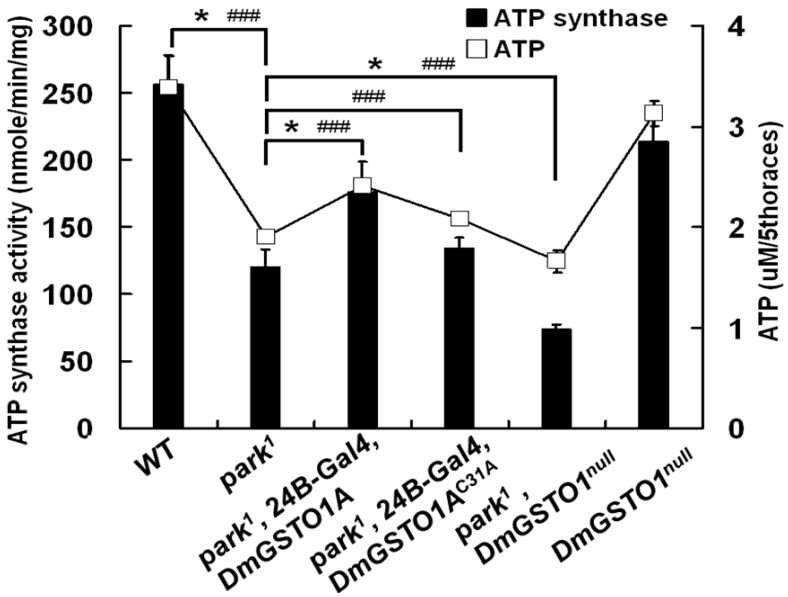

Figure 29. DmGSTO1 partially restored mitochondrial F_1F_0-ATP synthase activity and ATP level in *park*^{1} mutants.

Mitochondrial F_1F_0-ATP synthase activity and ATP levels in *Drosophila* thoraces. DmGSTO1A expression enhances ATP synthase activity and ATP levels of *park*^{1} mutants. *Error bars* indicate the standard deviation (S.D.). One-way ANOVA was used for statistical analysis (ATP synthase activity: *, $p < 0.05$; ATP level: ###, $P < 0.001$). Experiments were performed in triplicate.

8. Decreased ATP synthase subunit in *Drosophila* muscle leads to *park*^{1} mutant-like phenotype.

Mutations of ATP synthase subunits are known to exhibit mitochondrial dysfunction and neuromuscular impairment (Celotto *et al.*, 2006; Mayr *et al.*, 2010). To determine whether decreased ATP synthase activity was directly linked to the phenotypes found in *parkin* mutants, we down-regulated the ATP synthase β subunit in *Drosophila* thorax muscle using a UAS-RNAi line together with the muscle-specific *24B-Gal4* driver. Because the ATP synthase β subunit knockdown flies reared at 25 ℃ displayed pupal lethality, we performed all knockdown experiments at 18 ℃ to increase adult viability. When ATP synthase β subunit knockdown was induced at 18 ℃ in muscle using *24B-Gal4*, fewer than 20% of the flies were able to eclose. The ATP synthase β subunit RNAi flies showed accumulation of total α/β-tubulin (Figure 30A). Moreover, we observed abnormal muscle structure in the knockdown mutant flies, similar to the phenotypes found in *parkin* mutants (Figure 30B, C, red arrows; magnified view, Figure 30B' and C'). These results demonstrate that loss of the ATP synthase β subunit induces some of the *parkin* mutant phenotypes, including muscle degeneration and accumulation of tubulin.

Next, to examine whether the ATP synthase β subunit RNAi enhances the *parkin* mutant phenotype, the ATP synthase β subunit was knocked down in *park*^{1} mutant muscles. As shown in Figure 31A, we observed an increase in α/β-tubulin accumulation.

Figure 30. Muscle-specific ATP synthase β subunit RNAi

(A) Western blot analysis of adult thorax extracts from the ATP synthase β subunit RNAi mutant flies. α- and β-tubulin showed significant accumulation in the RNAi mutant muscle. (B and C) Muscle morphology of wild-type and ATP synthase β subunit RNAi mutant flies (red arrows, muscle degeneration; B’ and C’, magnified views). Muscle-specific ATP synthase β subunit RNAi resulted in degeneration of the flight muscles.

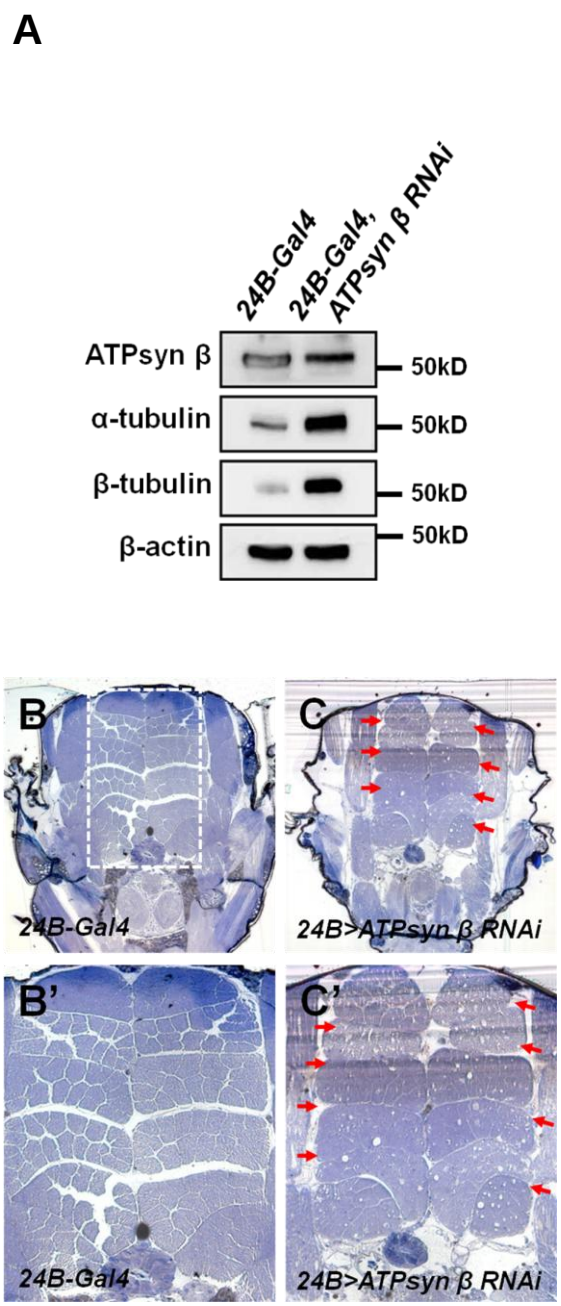
A
24B-Gal4
24B-Gal4, ATPsyn β RNAi
ATPsyn β
α-tubulin
β-tubulin
β-actin
50kD
50kD
50kD
50kD
B
C
24B-Gal4
24B>ATPsyn β RNAi
B'
C'
24B-Gal4
24B>ATPsyn β RNAi

Figure 31. Muscle-specific ATP synthase β subunit RNAi in *park*^{1} mutant background

(A) Western blot analysis of adult thorax extracts from the ATP synthase β subunit RNAi in a *park*^{1} mutant background. Accumulation of tubulin was increased more in the RNAi mutants than in the *park*^{1} single mutants. *Error bars* indicate the standard deviation (S.D.). The significance was determined by one-way ANOVA (**, $p < 0.01$; *, $P < 0.05$). (B) Western blot analysis of Hsp70/Hsc70, phosphorylated eIF2α, and total eIF2α (*, nonspecific band). The experimental significance was determined by one-way ANOVA (*, $p < 0.01$). β-actin was used as a loading control. Experiments were performed in triplicate.

A

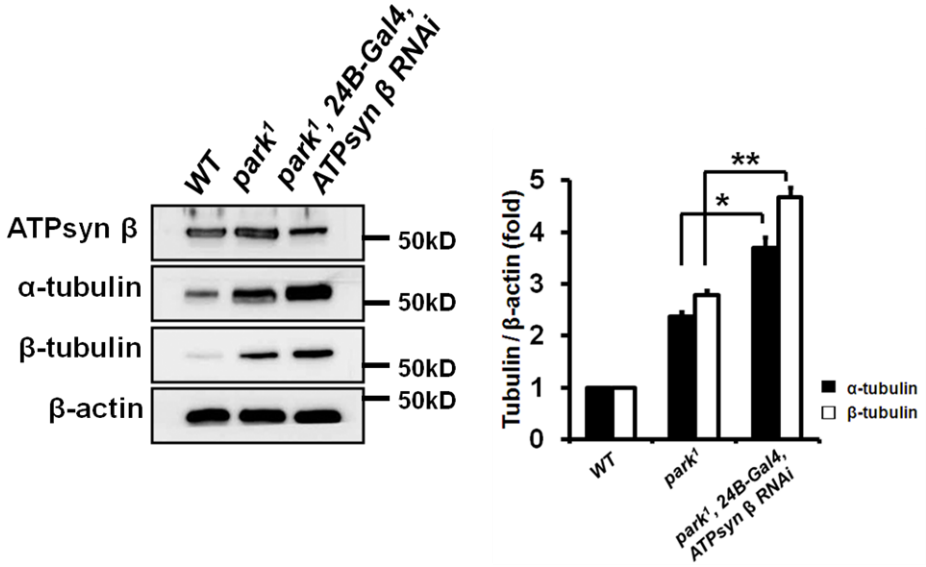
WT
park1
park1, 24B-Gal4, ATPsyn β RNAi
ATPsyn β
α-tubulin
β-tubulin
β-actin
50kD
50kD
50kD
50kD
Tubulin / β-actin (fold)
0
1
2
3
4
5
*
**
α-tubulin
β-tubulin
WT
park1
park1, 24B-Gal4, ATPsyn β RNAi

B

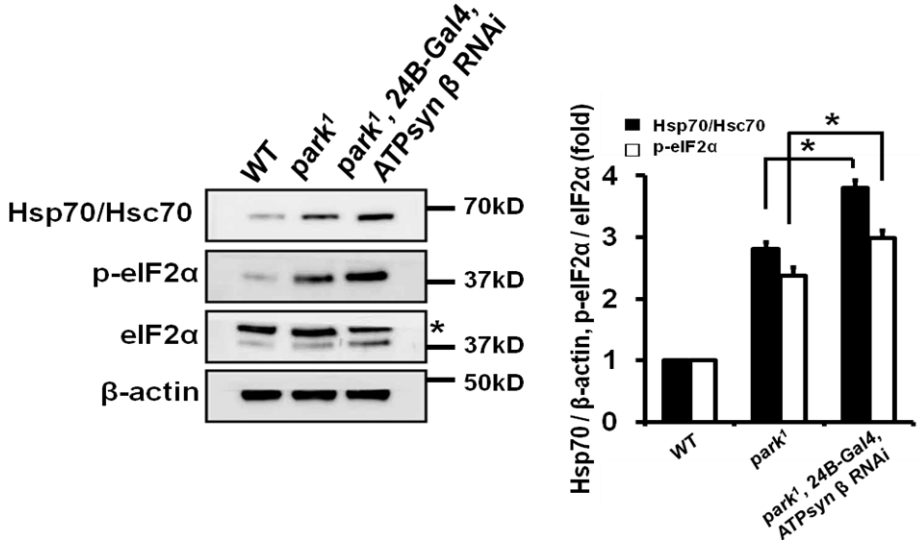
WT
park1
park1, 24B-Gal4, ATPsyn β RNAi
Hsp70/Hsc70
p-eIF2α
eIF2α
β-actin
70kD
37kD
*
37kD
50kD
Hsp70/Hsc70
p-eIF2α
Hsp70 / β-actin, p-eIF2α / eIF2α (fold)
0
1
2
3
4
*
*
WT
park1
park1, 24B-Gal4, ATPsyn β RNAi

Moreover, the levels of Hsp70/Hsc70 and phosphorylated eIF2α in the *park*^{1} mutant were further increased by RNAi knockdown of the ATPsynthase β subunit (Figure 31B). These data indicate that down-regulation of ATP synthase activity in the *park*^{1} mutant results in a more severe phenotype compared with that of *park*^{1} single mutants.

9. DmGSTO1 rescues mitochondrial ATP synthase assembly in *park*^{1} mutants.

To investigate how expression of DmGSTO1A affects ATP synthase activity, we examined the assembly level of the F_1F_0-ATP synthase complex (Complex V) by blue native PAGE and Western blot analysis with an anti-ATP synthase α subunit antibody. Mitochondrial F_1F_0-ATP synthase (Complex V) in *Drosophila* is a large multiprotein complex composed of eight different subunits, α, β, γ, δ, ε, a, b, and c (Figure 32A). Three bands (supercomplex, >800 kDa; assembled ATP synthase, Complex V, >600 kDa; F1 subcomplex, >400 kDa) were detected (Figure 32B, arrows). All three bands associated with the mitochondrial F_1F_0-ATP synthase complex were dramatically decreased by RNAi knockdown of the ATP synthase β subunit (Figure 32B). The amount of assembled ATP synthase was normalized using mitochondrial prohibitin. In comparison with the wild-type, the amount of assembled ATP synthase complex was decreased in *park*^{1} mutants. Expression of DmGSTO1A in *park*^{1} mutants increased the amount of assembled ATP synthase complex (Figure 33A, Complex V). Interestingly, *park*^{1}/*DmGSTO1*^{null} double mutants tend to exhibit lower amounts of assembled ATP

synthase than those in *park*^{1} mutants, although the effect was not statistically significant (Figure 33B). Blue native electrophoresis analysis is not sensitive to small changes; nevertheless, the change in the amount of assembled ATP synthase complex correlated to the change in ATP synthase activity. These results indicate that DmGSTO1A affects mitochondrial ATP synthase activity by regulating the assembly efficiency of ATP synthase in *park*^{1} mutants.

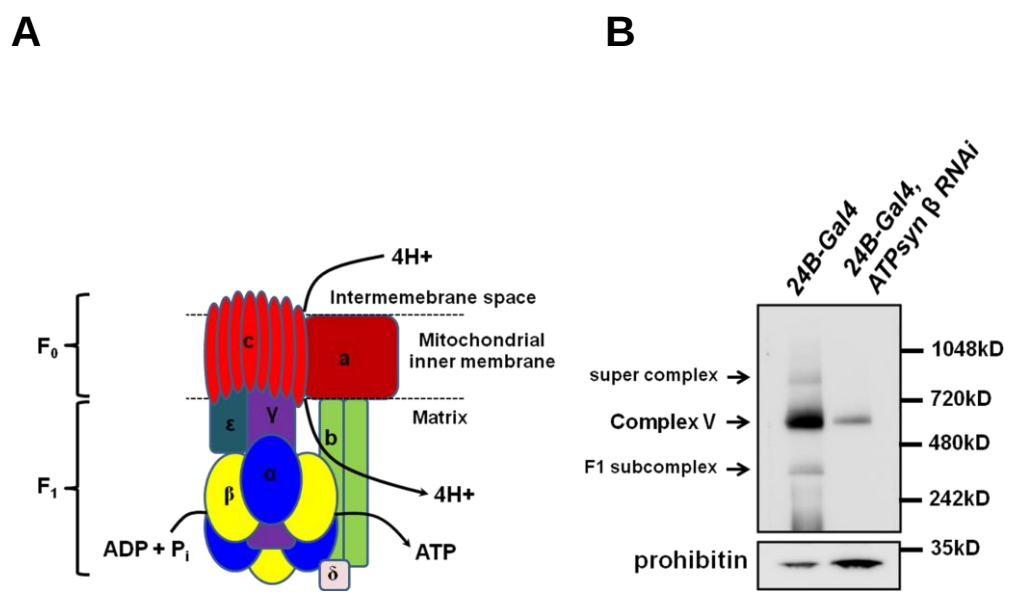

Figure 32. Mitochondrial F_1F_0-ATP synthase (Complex V) assembly in the ATP synthase β subunit RNAi mutants

(A) Mitochondrial F_1F_0-ATP synthase (Complex V) in *Drosophila* is a large multiprotein complex composed of eight different subunits. (B) Mitochondrial protein extracts from the thorax of adult flies were subjected to blue native PAGE, followed by western blot analysis with anti-ATP synthase α subunit antibody. Three bands were detected: supercomplex (>800 kDa), assembled ATP synthase (Complex V, >600 kDa), and F1 subcomplex (>400 kDa). All bands were decreased in the ATP synthase β subunit RNAi mutants. Prohibitin was used as a mitochondrial loading control.

Figure 33. Mitochondrial F_1F_0-ATP synthase (Complex V) assembly is affected by DmGSTO1 expression in *park*^{1} mutants.

(A and B) Mitochondrial protein extracts from the thorax of mutant fly lines were subjected to blue native PAGE, followed by western blot analysis with anti-ATP synthase α subunit antibody. Prohibitin was used as a mitochondrial loading control. (A) The assembly of ATP synthase (Complex V) was significantly decreased in *park*^{1} mutants. The amount of assembled ATP synthase was restored by DmGSTO1A up-regulation in *park*^{1} mutants. *Error bars* indicate the standard deviation (S.D.). The experimental significance was determined by one-way ANOVA (**, $p < 0.01$; *, $P < 0.0001$). Experiments were performed in quintuplicate. (B) The amount of assembled ATP synthase tended to decrease more in *park*^{1}*/DmGSTO1*^{null} double mutants than *park*^{1} mutants; however, the effect was not statistically significant. The significance was determined by one-way ANOVA (**, $p < 0.0001$; *, $P < 0.001$; ns, not significant). Experiments were performed in quadruplicate.

A

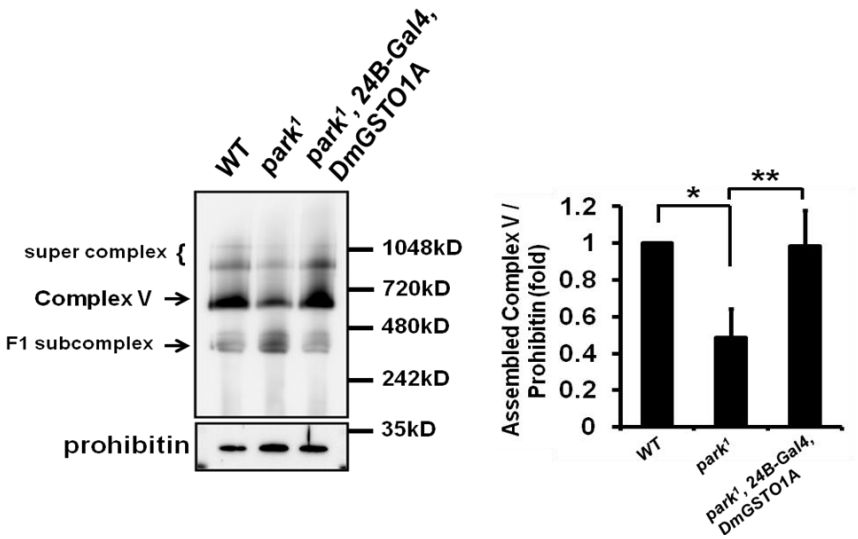
WT
park1
park1, 24B-Gal4, DmGSTO1A
super complex
Complex V
F1 subcomplex
prohibitin
1048kD
720kD
480kD
242kD
35kD
Assembled Complex V / Prohibitin (fold)
1.2
1
0.8
0.6
0.4
0.2
0
*
**
WT
park1
park1, 24B-Gal4, DmGSTO1A

B

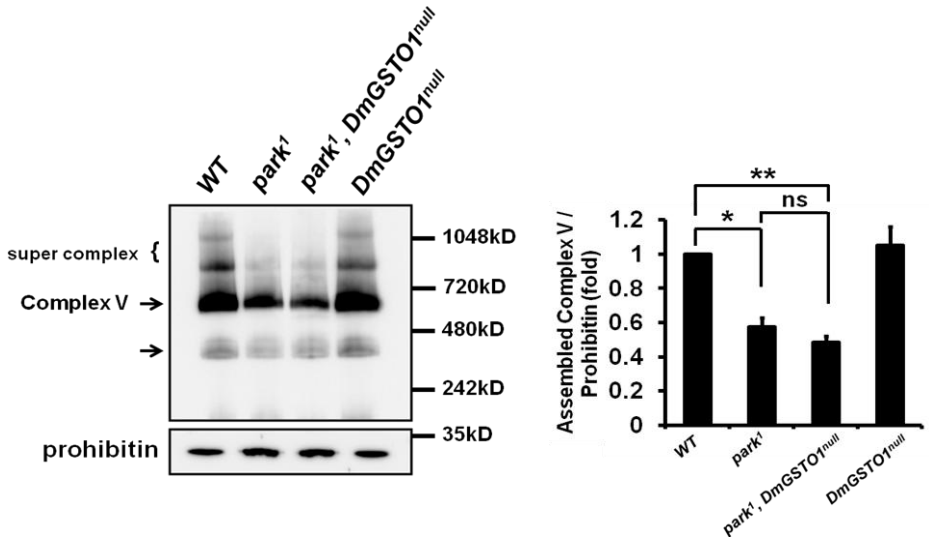
WT
park1
park1, DmGSTO1null
DmGSTO1null
super complex
Complex V
prohibitin
1048kD
720kD
480kD
242kD
35kD
Assembled Complex V / Prohibitin (fold)
1.2
1
0.8
0.6
0.4
0.2
0
**
*
ns
WT
park1
park1, DmGSTO1null
DmGSTO1null

10. The endogenous levels of the glutathionylated form of the ATP synthase β subunit in the thorax extracts were decreased in *PINK1^{B9}* mutants.

The loss of two genes, *parkin* and *PTEN-induced putative kinase 1* (*PINK1*), results in early-onset autosomal recessive parkinsonism (Kitada *et al.*, 1998; Valente *et al.*, 2004). PINK1 is a Ser/Thr kinase containing a mitochondrial targeting motif (Valente *et al.*, 2004). Cell culture studies reported that PINK1 overexpression can prevent the subsequent activation of caspase-3 under apoptotic stress conditions and reduction of PINK1 by RNAi increased neuronal toxicity from the dopaminergic neurotoxin, MPTP (Petit *et al.*, 2005; Haque *et al.*, 2008). Previous studies reported that mutations of *PINK1* lead to muscle degeneration, DA neuron loss, and mitochondrial dysfunction. PINK1 and parkin are linked in the same pathway, and PINK1 acts upstream of parkin (Park *et al.*, 2006; Deng *et al.*, 2008; Poole *et al.*, 2008; Yang *et al.*, 2008; Clark *et al.*, 2006). We therefore hypothesized that DmGSTO1A would genetically interact with the *PINK1* null mutant *PINK1^{B9}*. Interestingly, consistent with *park^{1}* mutants, we found that *DmGSTO1* and *parkin* mRNA were decreased in *PINK1^{B9}* mutants (Figure 34A). Glutathionylation of the mitochondrial ATP synthase β subunit was significantly decreased in *PINK1^{B9}* mutants (Figure 34B). Therefore, it seems possible that DmGSTO1A up-regulation may also contribute to the prevention of degeneration in *PINK1^{B9}* mutants.

To clarify the effect of DmGSTO1A on *PINK1^{B9}* mutants, we conducted a genetic study with *PINK1^{B9}* mutants (Figure 35). As shown in Figure 35D, up-regulation of DmGSTO1A under the control of a muscle-specific *Mef-Gal4* driver significantly

rescued the collapsed thorax phenotypes in *PINK1*^{B9} mutants. Degeneration of thorax muscles in *PINK1*^{B9} mutants occurs through apoptosis (Figure 36A and B). The thorax muscles in *PINK1*^{B9} mutants were subjected to a TUNEL assay. The increased TUNEL signal in *PINK1*^{B9} mutants was suppressed by DmGSTO1A expression (Figure 36C). These results indicate that DmGSTO1 has a protective effect in *PINK1*^{B9} mutants, and that DmGSTO1 interacts with the PINK1/Parkin pathway in *Drosophila*.

A

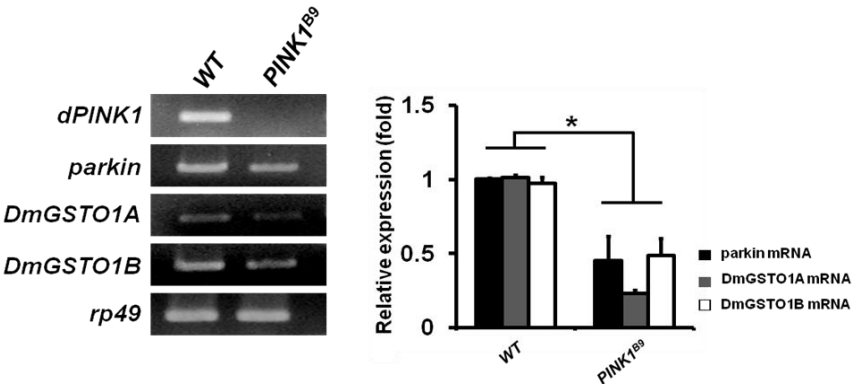

B

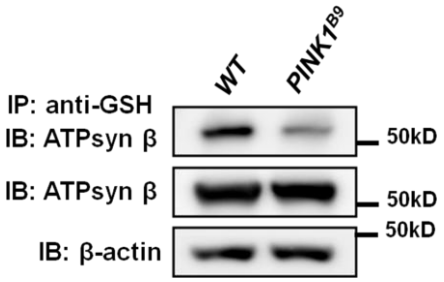

Figure 34. The endogenous levels of the glutathionylated form of the ATP synthase β subunit were decreased in *PINK1*^{B9} mutants.

(A) *parkin* and *DmGSTO1* mRNA levels were also reduced in the *PINK1*^{B9} mutants. *Error bars* indicate the standard deviation (S.D.). Experimental significance was determined by one-way ANOVA (*, $p < 0.05$). Experiments were performed in triplicate. (B) The levels of the glutathionylated ATP synthase β subunit were unchanged in *PINK1*^{B9} mutants. β-actin was used as a loading control.

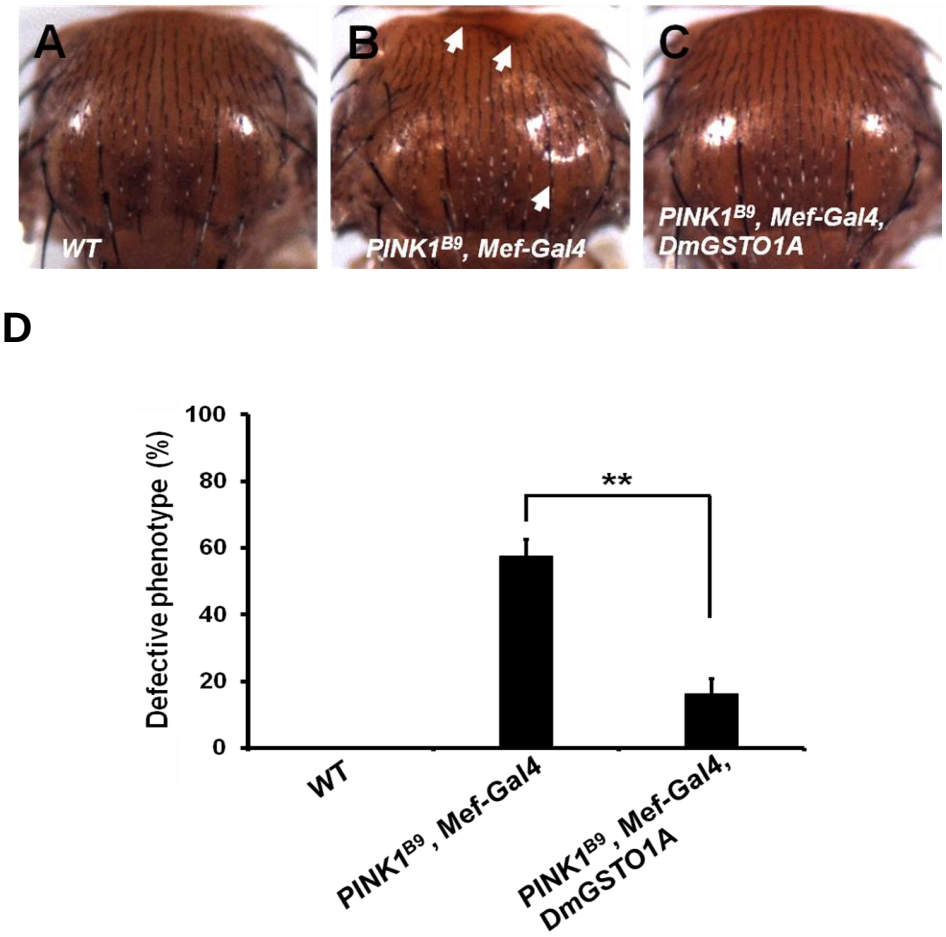

Figure 35. Up-regulation of DmGSTO1 rescues the thorax defect phenotype in *PINK1*^{B9} mutants.

(A-C) The collapsed thorax caused by *PINK1* loss-of-function (white arrows). (D) Statistical analysis of the percentage of 3-day-old flies with the collapsed thorax (n > 140) phenotype. The significance was determined by one-way ANOVA (**, $p < 0.01$).

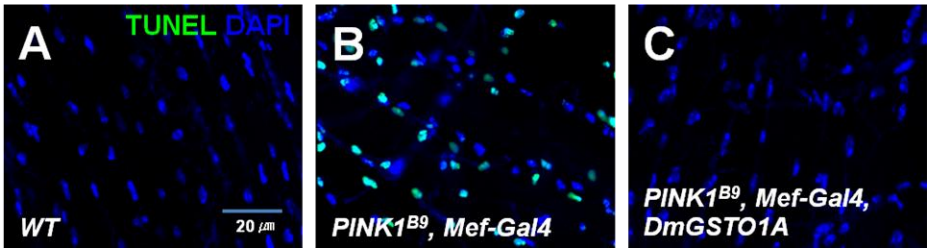

Figure 36. Overexpression of DmGSTO1 restores the apoptotic cell death in *PINK1*^{B9} mutant muscles.

(A-C) Merged images of apoptotic cells (TUNEL, green) and nuclei (DAPI, blue). Apoptosis in *PINK1*^{B9} mutant thoraces is reduced by DmGSTO1A expression.

IV. Discussion

In this study, we suggest that DmGSTO1 is a novel genetic suppressor of parkin dysfunction and has a protective role in a model of PD. Moreover, we showed that the ATP synthase β subunit is a novel target of DmGSTO1 in *Drosophila*. The ATP synthase β subunit is an essential catalytic core component of the F_1F_0-ATP synthase complex in mitochondria. We found that levels of glutathionylation of the ATP synthase β subunit were significantly decreased in *park*^{1} mutants, whereas its total protein level remained unchanged. Glutathionylation is a mechanism of post-translational regulation of several proteins, including protein-tyrosine phosphatase 1B (PTP1B), and MEKK1. The glutathionylation of a calcium channel, ryanodine receptor 1 (RyR1), activates it and enhances calcium release (Hidalgo *et al.*, 2006). Our results suggest that expression of DmGSTO1A in *park*^{1} mutants increases the level of glutathionylated ATP synthase β subunit and restores mitochondrial F_1F_0-ATP synthase activity, thereby partially rescuing *park*^{1} mutant phenotypes, including the degeneration of DA neurons.

The increase in F_1F_0-ATP synthase activity and assembly by DmGSTO1A in the *park*^{1} mutant led to a recovery of ATP depletion. Interestingly, because mitochondrial F_1F_0-ATP synthase has a role in maintaining inner membrane morphology, and mitochondrial membrane potential (Celotto *et al.*, 2006; Brown *et al.*, 2006) and mutation of F_1F_0-ATP synthase ε subunit can cause mitochondrial dysfunction (Mayr *et al.*, 2010), the restoration of F_1F_0-ATP synthase activity in the *park*^{1} mutant is

important for rescuing the *parkin* mutant phenotypes. Moreover, RNAi mutants of the ATP synthase β subunit exhibit phenotypes similar to *park*^{1} mutants, including α/β-tubulin accumulation, locomotor dysfunction, UPR activation, and muscle degeneration.

Although the change in mitochondrial F_1F_0-ATP synthase activity and ATP levels correlated with the degree of glutathionylation of the ATP synthase β subunit, the exact regulatory mechanism between glutathionylation of the ATP synthase β subunit and ATP synthase activity is not known. It is technically difficult to show a direct relationship between glutathionylation of the ATP synthase β subunit and ATP synthase activity because in *Drosophila*, mitochondrial ATP synthase is a large multiprotein complex composed of eight different subunits. Further studies will be required to determine how glutathionylation of the ATP synthase β subunit regulates mitochondrial ATP synthase activity and assembly at the molecular level. However, the loss-of-function mutant *DmGSTO1*^{null} exhibited no obvious morphological defects and slightly reduced glutathionylation of the ATP synthase β subunit and ATP synthase activity. It is not clear why *DmGSTO1*^{null} single mutants show a weak effect on the glutathionylation and activity of ATP synthase. One possible explanation is that compensatory mechanisms related to glutathionylation of the ATP synthase β subunit exist *in vivo*.

Cysteine, methionine, tryptophan and tyrosine residues are the most oxidant sensitive and reversible and irreversible modifications have been characterized. Conjugation of GSH to tyrosine residues in proteins is a novel mechanism of protein-GSH formation (Nagy *et al*., 2012). The ATP synthase β subunit does not contain any

cysteine residues in its protein sequence. Possible glutathionylation mechanisms could be by posttranslational modification of several methionine residues into homocysteine (Figure 37). To search for potential methionine targets for glutathionylation within the ATP synthase β subunit, we subjected glutathionylated ATP synthase β subunit to digestion and liquid chromatography-tandem mass spectrometry (LC-MS/MS) analysis. Peptides with a mass difference of about 307 Da, representing one GSH, were detected by LC-MS/MS. We identified four glutathionylated methionine residues, Met^{194}, Met^{249}, Met^{316}, and Met^{319} (Figure 38). We found that Met^{194} and Met^{249} are located at the interaction interface with ATP synthase α subunit. Therefore, glutathionylation of these residues might be important to interact with ATP synthase α subunit. Although the exact mechanism by which glutathionylated ATP synthase β subunit regulates the ATP synthase complex assembly is not known, it would be expected to modulate physical interaction with other subunits. Further studies will be required to identify the exact glutathionylated site of ATP synthase β subunit.

Although our current study focused on the specific target of GSTO related to neurodegeneration, previous studies have shown that GSTs have protective functions against oxidative stress in neurodegenerative diseases. Loss-of-function of the yeast *GSTS1* homolog, *gtt-1*, enhances α-synuclein toxicity (Willingham *et al.*, 2003), and mouse GST Pi contributes to the sensitivity to xenobiotics in idiopathic PD (Smeyne *et al.*, 2007). Additionally, increased GST Pi expression protected cells from rotenone-induced neurotoxicity (Shi *et al.*, 2009). However, the various roles of GSTs remain controversial because of the diversity and complexity of these proteins.

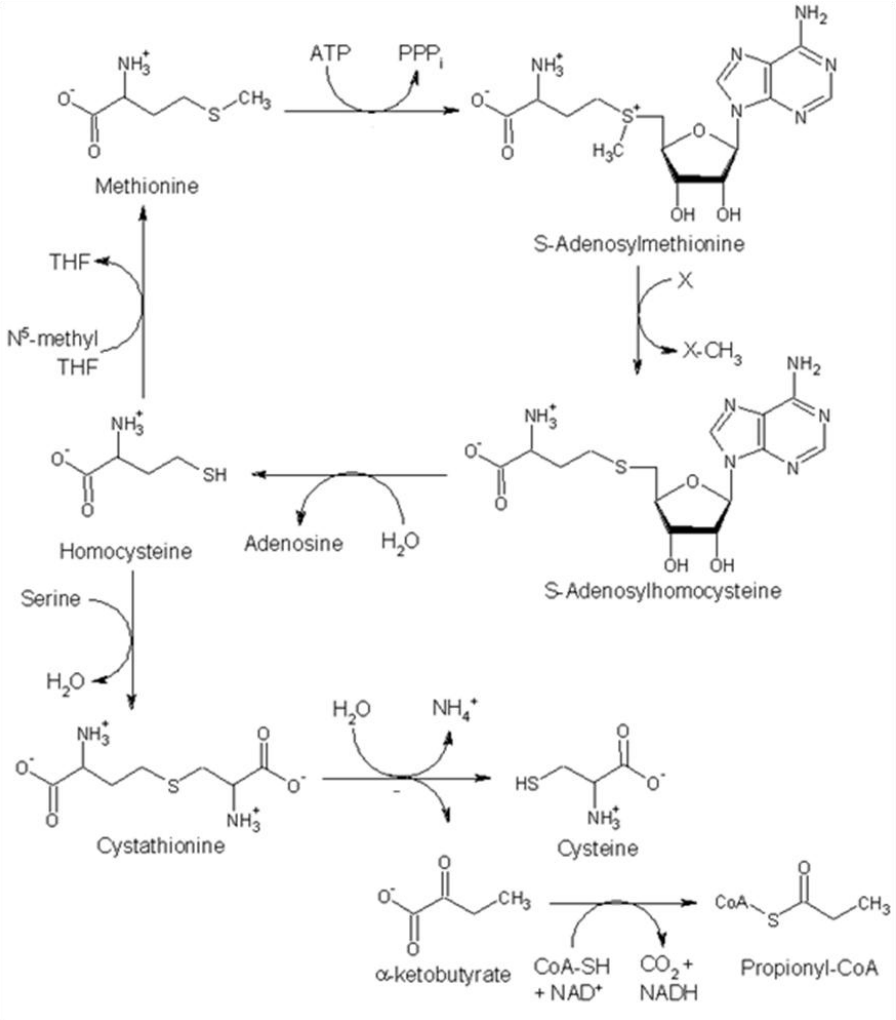

Figure 37. Methionine can be converted to homocysteine.

Homocysteine can be remethylated to methionine or transsulphurated to cystathionine and cysteine. Cysteine and methionine are sulfur-containing amino acids.

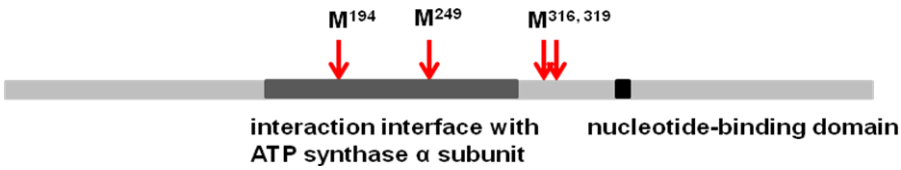

Figure 38. Identification of the potential glutathionylation sites of ATP synthase β subunit

Methionine 194, 249, 316 and 319 of ATP synthase β subunit are putative target amino acids for glutathionylation (arrows).

Because the expression levels of several GSTs increase due to oxidative stress, we measured endogenous DmGSTO1A expression in *park*^{1} mutants and found that the protein and mRNA levels of DmGSTO1A were significantly lowered in *park*^{1} mutants. Transcriptional profiling of *parkin* mutants showed that the oxidative stress response genes are up-regulated, and overexpression of GSTS1 in DA neurons suppressed neurodegeneration in *parkin* mutants (Greene *et al.*, 2005; Whitworth *et al.*, 2005). DmGSTS1 was also up-regulated by the 4E-BP1-mediated stress response (Tain *et al.*, 2009). Therefore, DmGSTS1 in *park*^{1} mutants may be increased in an effort to decrease the stress induced by the *parkin* mutation, but its increased level is not sufficient to rescue the *park*^{1} phenotype. Both DmGSTO1 mRNA and protein levels were decreased in *park*^{1} mutants, suggesting that the normal function of parkin is critical for the regulation of DmGSTO1 expression. Little is known about the factors regulating *DmGSTO1* gene expression, but we can make the following speculation. Because the *DmGSTO1* gene contains a potential NF-κB-like transcription factor binding motif (Li *et al.*, 2008), and parkin stimulates NF-κB-dependent transcription (Henn *et al.*, 2007), DmGSTO1 may be down-regulated in the *park*^{1} mutant (Figure 39). NF-κB transcription factor regulates several biological processes, including immunity, apoptosis. Thus, the mechanism underscoring the protective role of DmGSTO1 in *park*^{1} mutants is distinct from the mechanisms used by general antioxidants and the detoxifying enzyme DmGSTS1. Furthermore, GSTO1 has an active site cysteine residue, which is distinct from the tyrosine residue found in GSTS1. This cysteine residue could enable GSTO1 to modulate the disulfide status of cysteine residues on substrate proteins (Board *et al.*, 2000).

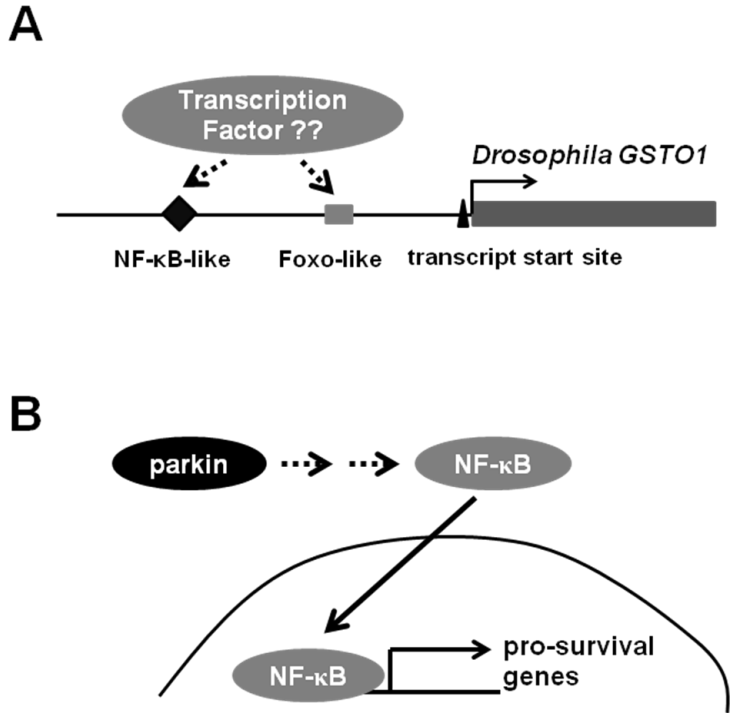

Figure 39. A model for the regulation of *DmGSTO1* gene expression by parkin

(A) Potential transcription factor binding motif of *Drosophila* GSTO1. *Drosophila* GSTO1 contained NF-κB-like and Foxo-like motif in 600bp and 200bp upstream of the gene transcription start site. (B) Under moderate stress, parkin stimulates NF-κB-dependent transcription. Therefore, transcription of pro-survival genes is up-regulated. Mutations in the *parkin* gene interfere with the ability of parkin to stimulate the NF-κB signaling pathway.

Although the specific substrates of individual GSTs remain unknown, the functional diversity of GSTs might explain why they have different substrates against various stresses *in vivo*.

DmGSTO1B more strongly protects against oxidative stress than DmGSTO1A, but only the up-regulation of DmGSTO1A improved the defective phenotypes in *parkin* mutants. Although DHAR activity and the reduced form of ascorbate have protective roles under oxidative stress conditions (Chen *et al.*, 2003), they are not sufficient to rescue *parkin* mutant phenotypes. As shown in Figure 26 and 27, DmGSTO1B was not able to glutathionylate the ATP synthase β subunit. Thus, we propose that these two isoforms, DmGSTO1A and DmGSTO1B, have different substrates and act differently on the stress response pathway *in vivo*.

Mitochondrial defects have been detected in PD cases with *parkin* mutations. Recent studies suggest that *parkin* promotes mitochondrial fission and/or inhibits mitochondrial fusion in muscle tissues and DA neurons (Deng *et al.*, 2008; Poole *et al.*, 2008; Yang *et al.*, 2008). Staining mitochondria with streptavidin revealed severe defects in mitochondrial integrity in the IFMs of $park^{1}$ mutants. Interestingly, these defects were not restored by DmGSTO1A expression, and $park^{1}/DmGSTO1^{null}$ double mutants were not distinguishable from $park^{1}$ single mutants (Figure 40A-D). These findings were further confirmed by expressing *mito-GFP* in thorax muscles (Figure 40F-I). In contrast to the $park^{1}$ mutants, the ATP synthase β subunit RNAi mutants did not show disrupted mitochondrial morphology (Figure 40A and E). These results suggest that DmGSTO1 is not important for restoring mitochondrial morphology in $park^{1}$ mutants and might act downstream or in parallel to the mitochondrial dynamics.

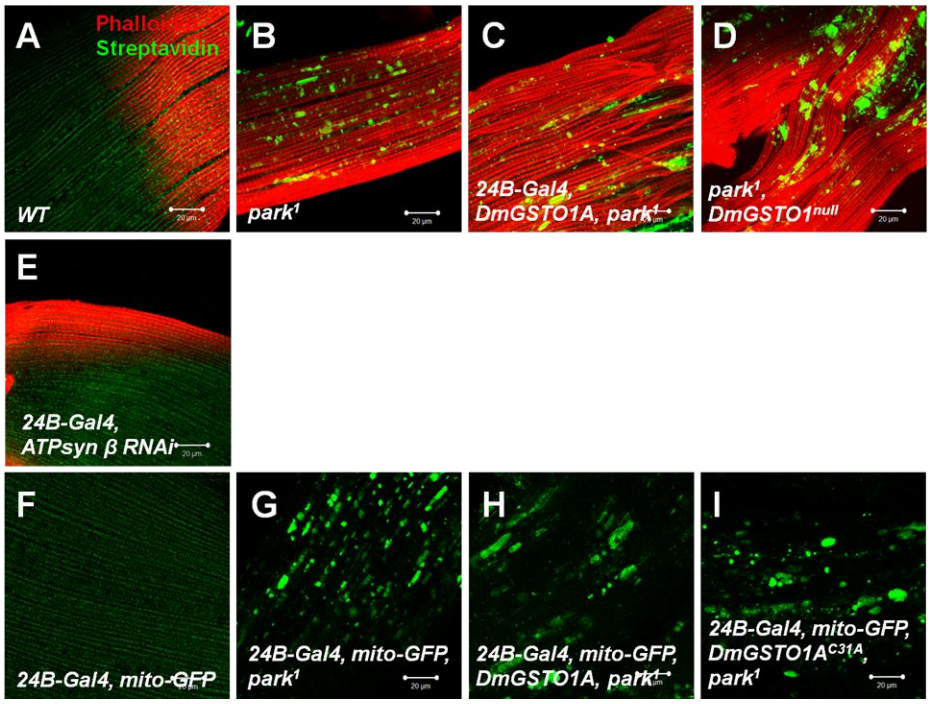

Figure 40. DmGSTO1 is not important for the suppression of mitochondrial morphological defects in *park*^{1} mutants.

(A-E) Mitochondria in flight muscle were stained with Alexa 488-conjugated streptavidin. Compared with wild-type, *park*^{1} mutants displayed large clumps of intense signal. Up-regulation of DmGSTO1A in *park*^{1} mutants did not suppress either the *park*^{1} mutant phenotype or the mitochondrial morphological defects. ATP synthase β subunit RNAi mutants also displayed normal mitochondrial morphology. (F-I) Mitochondria in IFM tissues of *Drosophila* thorax were labeled by *mito-GFP*. Compared with *park*^{1} mutant, DmGSTO1A or DmGSTO1A^{C31A} expressing lines in a *park*^{1} mutant background also showed mitochondrial morphological defects.

The most important aim of the GST research field is to define the physiological function of GSTs. However, particularly in multigene families of GST enzymes where functional redundancy is common, it is difficult to define the function of GSTs, as other GSTs can compensate for the loss of function. Although the *DmGSTO1*^{null} single mutation exhibited no significant reduction in the glutathionylation of the ATP synthase β subunit and ATP synthase activity, mutations of DmGSTO1 with parkin enhanced the *park*^{1} mutant phenotypes with more severely reduced ATP synthase activity (Figure 27 and 29). More than 36 GST genes are present in *Drosophila* (Ranson *et al*., 2001), and they may have partially overlapping functions. Several cases of redundancy amongst GSTs have been reported, and the functional redundancy of GSTO1 might explain the slightly decreased glutathionylation of the ATP synthase β subunit and ATP synthase activity in *DmGSTO1*^{null} single mutants. Although functional redundancy of a glutathionylating enzyme may account for the slight phenotype observed in *DmGSTO1*^{null} single mutants, it is difficult to determine which one of them is the major contributor. It is also possible that glutathionylating enzymes could supplement each other. No other enzymes are known to be involved in the glutathionylation of the ATP synthase β subunit except DmGSTO1.

Glutathionylation is the post-translational modification of protein by the addition of a glutathione (GSH). It has the potential to alter protein structures and induces functional change in the target proteins. This modification is controlled by the GST, thioredoxin (Trx) and glutaredoxin (Grx) system (Anathy *et al*., 2009; Gallogly *et al*., 2007; Reynaert *et al*., 2006). Grx comprise the thioredoxin (Trx) superfamily of thioltransferases and a common active site motif, Cys-X-X-Cys. DmGSTO1 also has a

Trx-like fold in its N-terminus, and multifunctional properties displaying Grx/Trx features (Kim *et al*., 2006). These putative glutathionylating enzymes are functionally conserved in *Drosophila*. In *Drosophila*, there are eleven *Trx* homologue gene, *CG8517*, *CG8993*, *CG3719*, *CG13473*, *Trx-2*, *TrxT*, *Trx-1*, *Txl*, *Trxr-1*, *Trxr-2*, *CG10157*, and four *Grx* homologue genes, *Clot*, *Grx-1*, *CG6523*, and *CG6852* (Svnsson *et al*., 2007; Tsuda *et al*., 2010). To investigate the transcription levels of putative glutathionylating enzymes, we determined the expression levels of several *Trx* and *Grx* homologues in *DmGSTO1*^{null} mutants using real-time PCR. Interestingly, as shown in Figure 41, we found one up-regulated (*Trxr-2*), and three down-regulated (*TrxT*, *Trxr-2* and *CG10157*) *Trx* homologues as well as one down-regulated (*Grx-1*) *Grx* homologue in *DmGSTO1*^{null} mutants. We also hypothesized that the expression of these functionally redundant enzymes, which are *Trx* and *Grx* homologues, is reduced in *park*^{1} mutants. As shown in Figure 41, we observed two up-regulated (*CG8517* and *TrxT*), and one down-regulated (*Trxr-2*) *Trx* homologue as well as two up-regulated (*Clot* and *Grx-1*) *Grx* homologues in *park*^{1} mutants. However, *CG8517*, *TrxT* and *Grx-1* transcripts are primarily expressed in male flies and Clot is required for the synthesis of eye color pigment in *Drosophila*. Therefore, we excluded these genes as a candidate for glutathionylating enzymes. Interestingly, one of the candidate genes, *Trxr-2* transcript is up-regulated in *DmGSTO1*^{null} mutants and down-regulated in *park*^{1} mutants. It seems that expression of putative glutathionylating enzymes tend to up-regulate in *DmGSTO1*^{null} mutants. These results suggest that the compensatory mechanism of the glutathionylating system for specific target proteins (such as ATP synthase β subunit) may be up-regulated in *DmGSTO1*^{null} mutants.

Figure 41. Validation of gene expression using real-time RT-PCR in *DmGSTO1*^{null} and *park*^{1} mutants

(A) The expression profile of *Trxr-2* shown a significant induction while *TrxT*, *Trxr-1* and *CG10157* were significantly reduced in *DmGSTO1*^{null} mutants. Error bars indicate standard deviation. The experimental significance was determined by one-way ANOVA (**, $p < 0.05$; ***, $P < 0.01$). (B) The expression profile of *Trxr-2* showed a significant reduction while *CG8517*, *TrxT*, *Clot* and *Grx-1* were significantly induced in *park*^{1} mutants. The results were plotted as fold differences of relative gene expression normalized to the wild type controls. Error bars indicate standard deviation. The experimental significance was determined by one-way ANOVA (*, $p < 0.05$; **, $p < 0.01$; ***, $P < 0.001$). Experiments were performed in triplicate.

A

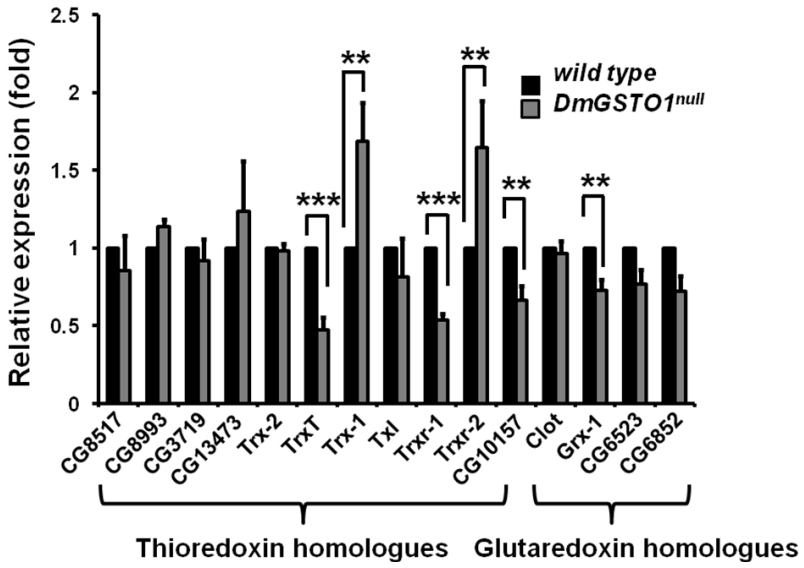
Relative expression (fold)
2.5
2
1.5
1
0.5
0
wild type
DmGSTO1null
**
**
**
***
***
**
**
CG8517
CG8993
CG3719
CG13473
Trx-2
TrxT
Trx-1
Txl
Trxr-1
Trxr-2
CG10157
Clot
Grx-1
CG6523
CG6852
Thioredoxin homologues
Glutaredoxin homologues

B

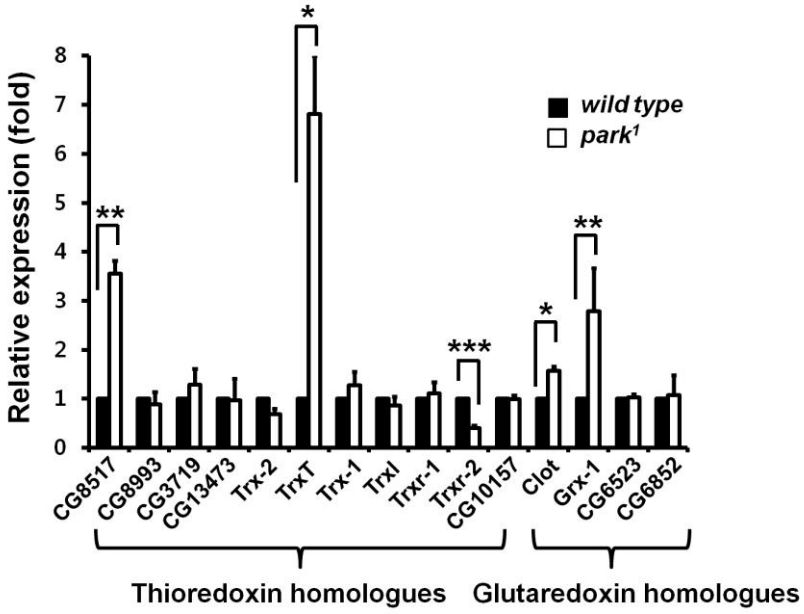
Relative expression (fold)
8
7
6
5
4
3
2
1
0
wild type
park1
*
**
**
*
***
CG8517
CG8993
CG3719
CG13473
Trx-2
TrxT
Trx-1
Txl
Trxr-1
Trxr-2
CG10157
Clot
Grx-1
CG6523
CG6852
Thioredoxin homologues
Glutaredoxin homologues

The up-regulation of this putative glutathionylating enzyme, *Trxr-2* might also explain the slightly decreased glutathionylation of the ATP synthase subunit in *DmGSTO1*^{null} single mutants. These results suggest that the compensatory mechanism of putative glutathionylating enzymes may be down-regulated in *park*^{1} mutants. Further studies will be required to research the compensatory mechanism of the glutathionylating system for ATP synthase β subunit.

Our results support the hypothesis that DmGSTO1 is linked to the pathogenic phenotypes displayed in *parkin* mutants. We found that DmGSTO1 is a novel genetic suppressor of parkin dysfunction. The two isoforms of DmGSTO1 have different functions. DmGSTO1B in *Drosophila* is required to protect the flies against oxidative stress. Although the exact molecular mechanism is not clear, glutathionylation of the ATP synthase β subunit by DmGSTO1A regulates mitochondrial F_1F_0-ATP synthase activity, and the restoration of ATP synthase activity by DmGSTO1A expression is critically important for partial rescue of the mitochondrial function in *park*^{1} mutants (Figure 42). These findings present a novel mechanism of regulation of ATP synthase by DmGSTO1 in *parkin* mutants. Our results strongly suggest that promoting DmGSTO1 activity could alleviate neurodegeneration in *parkin* mutants. These findings will lead us to a better understanding of the molecular mechanism of neuroprotection due to GSTO in PD and could help in developing new therapeutic approaches for PD.

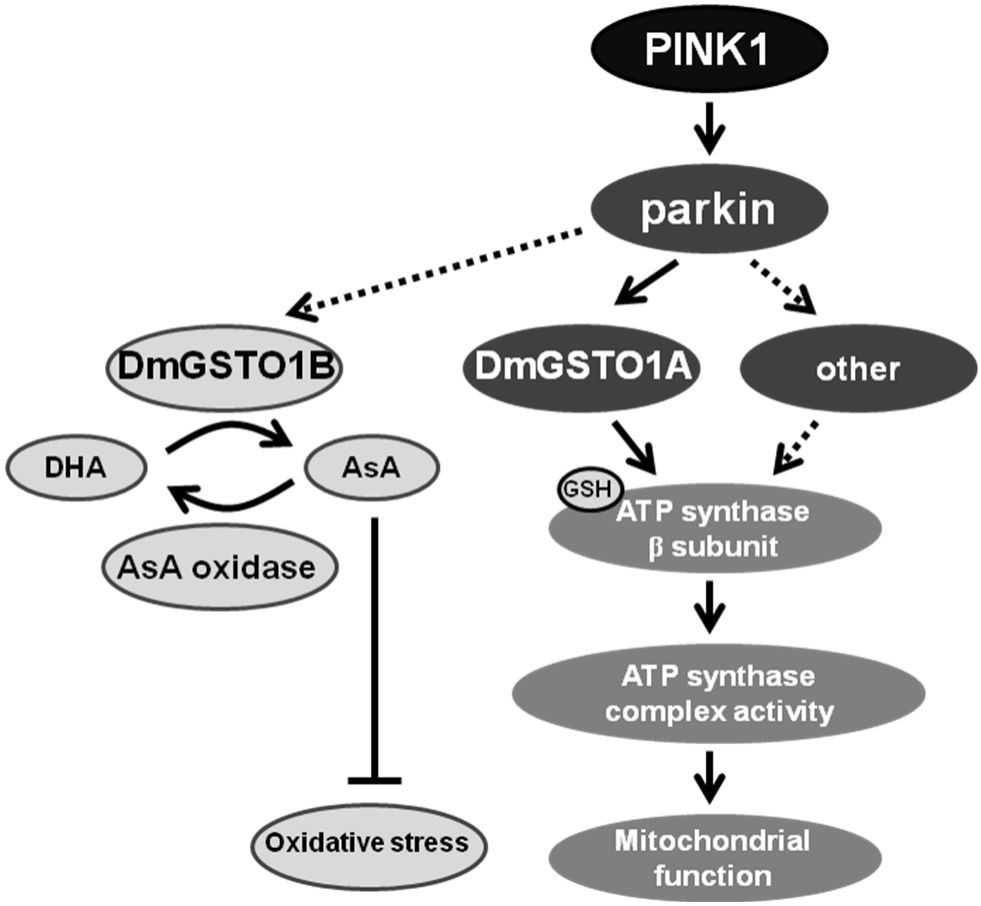

Figure 42. Proposed model for the role of *Drosophila* GSTO1

See discussions for detail.

V. References

Abou-Sleiman, P. M., Muqit, M. M., and Wood, N. W. (2006) Expanding insights of mitochondrial dysfunction in Parkinson's disease. *Nat. Rev. Neurosci.* 7, 207–219

Adachi, T., Weisbrod, R. M., Pimentel, D. R., Ying, J., Sharov, V. S., Schoneich, C., and Cohen, R. A. (2004) *S*-Glutathiolation by peroxynitrite activates SERCA during arterial relaxation by nitric oxide. *Nat. Med.* 10, 1200–1207

Anathy, V., Aesif, S. W., Guala, A. S., Havermans, M., Reynaert, N. L., Ho, Y. S., Budd, R. C., and Janssen-Heininger Y. M. (2009) Redox amplification of apoptosis by caspase-dependent cleavage of glutaredoxin 1 and S-glutathionylation of Fas. *J. Cell. Biol.* 184, 241–252

Board, P. G., Coggan, M., Chelvanayagam, G., Easteal, S., Jermiin, L. S., Schulte, G. K., Danley, D. E., Hoth, L. R., Griffor, M. C., Kamath, A. V., Rosner, M. H., Chrunyk, B. A., Perregaux, D. E., Gabel, C. A., Geoghegan, K. F., and Pandit, J. (2000) Identification, characterization, and crystal structure of the omega class glutathione transferases. *J. Biol. Chem.* 275, 24798–24806

Brown, S. V., Hosking, P., Li, J., and Williams, N. (2006) ATP synthase is responsible for maintaining mitochondrial membrane potential in bloodstream form

Trypanosoma brucei. *Eukaryot. Cell* 5, 45–53

Capaldi, R. A., and Aggeler, R. (2002) Mechanism of the F_1F_0-type ATP synthase, a biological rotary motor. *Trends Biochem. Sci.* 27, 154–160

Celotto, A. M., Frank, A. C., McGrath, S. W., Fergestad, T., Van Voorhies, W. A., Buttle, K. F., Mannella, C. A., and Palladino, M. J. (2006) Mitochondrial encephalomyopathy in *Drosophila*. *J. Neurosci.* 26, 810–820

Cha, G. H., Kim, S., Park, J., Lee, E., Kim, M., Lee, S. B., Kim, J. M., Chung, J., and Cho, K. S. (2005) Parkin negatively regulates JNK pathway in the dopaminergic neurons of *Drosophila*. *Proc. Natl. Acad. Sci. U.S.A.* 102, 10345–10350

Chen, Z., Young, T. E., Ling, J., Chang, S. C., and Gallie, D. R. (2003) Increasing vitamin C content of plants through enhanced ascorbate recycling. *Proc. Natl. Acad. Sci. U.S.A.* 100, 3525–3530

Chung, K. K., Zhang, Y., Lim, K. L., Tanaka, Y., Huang, H., Cao, J., Ross, C. A., Dawson V. L., and Dawson T. M. (2001) Parkin ubiquitinates the α-synuclein-interacting protein, synphilin-1: implications for Lewy-body formation in Parkinson disease. *Nat. Med.* 7, 1144–1150

Clark, I. E., Dodson, M. W., Jiang, C., Cao, J. H., Huh, J. R., Seol, J. H., Yoo, S. J.,

Hay, B. A., and Guo, M. (2006) *Drosophila* pink1 is required for mitochondrial function and interacts genetically with parkin. *Nature* 441, 1162–1166

Collinson, I. R., Skehel, J. M., Fearnley, I. M., Runswick, M. J., and Walker, J. E. (1996) The F_1F_0-ATPase complex from bovine heart mitochondria: the molar ratio of the subunits in the stalk region linking the F_1 and F_0 domains. *Biochemistry* 34, 12640–12646

Cross, R. L., and Muller, V. (2004) The evolution of A-, F-, and V-type ATP synthases and ATPases. Reversals in function and changes in the H^+/ATP coupling ratio. *FEBS Lett.* 576, 1–4

Dawson, T. M., and Dawson, V. L. (2003) Molecular pathways of neurodegeneration in Parkinson's disease. *Science* 302, 819–822

Deng, H., Dodson, M. W., Huang, H., and Guo, M. (2008) The Parkinson's disease genes pink1 and parkin promote mitochondrial fission and/or inhibit fusion in *Drosophila*. *Proc. Natl. Acad. Sci. U.S.A.* 105, 14503–14508

Dulhunty, A., Gage, P., Curtis, S., Chelvanayagam, G., and Board, P. (2001) The glutathione transferase structural family includes a nuclear chloride channel and a ryanodine receptor calcium release channel modulator. *J. Biol. Chem.* 276, 3319–3323

Friggi-Grelin, F., Coulom, H., Meller, M., Gomez, D., Hirsh, J., and Birman, S. (2003) Targeted gene expression in *Drosophila* dopaminergic cells using regulatory sequences from tyrosine hydroxylase. *J. Neurobiol.* 54, 618–627

Gallogly, M. M., and Mieyal, J. J. (2007) Mechanisms of reversible protein glutathionylation in redox signaling and oxidative stress. *Curr. Opin. Pharmacol.* 7, 381–391

Greene, J. C., Whitworth, A. J., Andrews, L. A., Parker, T. J., and Pallanck, L. J. (2005) Genetic and genomic studies of *Drosophila* parkin mutants implicate oxidative stress and innate immune responses in pathogenesis. *Hum. Mol. Genet.* 14, 799–811

Greene, J. C., Whitworth, A. J., Kuo, I., Andrews, L. A., Feany, M. B., and Pallanck, L. J. (2003) Mitochondrial pathology and apoptotic muscle degeneration in *Drosophila* parkin mutants. *Proc. Natl. Acad. Sci. U.S.A.* 100, 4078–4083

Haque, M. E., Thomas, K. J., D'Souza, C., Callaghan, S., Kitada, T., Slack, R. S., Fraser, P., Cookson, M. R., Tandon, A., and Park, D. S. (2008) Cytoplasmic Pink1 activity protects neurons from dopaminergic neurotoxin MPTP. *Proc. Natl. Acad. Sci. U.S.A.* 105, 1716–1721

Hayes, J. D., Flanagan, J. U., and Jowsey, I. R. (2005) Glutathione transferases. *Annu. Rev. Pharmacol. Toxicol.* 45, 51–88

Haynes, C. M., and Ron, D. (2010) The mitochondrial UPR. Protecting organelle protein homeostasis. *J. Cell Sci.* 123, 3849–3855

Henn, I. H., Bouman, L., Schlehe, J. S., Schlierf, A., Schramm, J. E., Wegener, E., Nakaso, K., Culmsee, C., Berninger, B., Krappmann, D., Tatzelt, J., and Winklhofer, K. F. (2007) Parkin mediates neuroprotection through activation of IκB kinase/nuclear factor-κB signaling. *J. Neurosci.* 27, 1868–1878

Hidalgo, C., Sanchez, G., Barrientos, G., and Aracena-Parks, P. (2006) A transverse tubule NADPH oxidase activity stimulates calcium release from isolated triads via ryanodine receptor type 1 *S*-glutathionylation. *J. Biol. Chem.* 281, 26473–26482

Hoopfer, E. D., Penton, A., Watts, R. J., and Luo, L. (2008) Genomic analysis of *Drosophila* neuronal remodeling. A role for the RNA-binding protein Boule as a negative regulator of axon pruning. *J. Neurosci.* 28, 6092–6103

Hoozemans, J. J., van Haastert, E. S., Eikelenboom, P., de Vos, R. A., Rozemuller, J. M., and Scheper, W. (2007) Activation of the unfolded protein response in Parkinson's disease. *Biochem. Biophys. Res. Commun.* 354, 707–711

Imai, Y., Soda, M., Inoue, H., Hattori, N., Mizuno, Y., and Takahashi, R. (2001)

An unfolded putative transmembrane polypeptide, which can lead to endoplasmic reticulum stress, is a substrate of Parkin. *Cell* 105, 891–902

Kim, J., Suh, H., Kim, S., Kim, K., Ahn, C., and Yim, J. (2006) Identification and characteristics of the structural gene for the *Drosophila* eye color mutant sepia, encoding PDA synthase, a member of the omega class glutathione *S*-transferases. *Biochem. J.* 398, 451–460

Kitada, T., Asakawa, S., Hattori, N., Matsumine, H., Yamamura, Y., Minoshima, S., Yokochi, M., Mizuno, Y., and Shimizu, N. (1998) Mutations in the parkin gene cause autosomal recessive juvenile parkinsonism. *Nature* 392, 605–608

Kuroda, Y., Mitsui, T., Kunishige, M., and Matsumoto, T. (2006) Parkin affects mitochondrial function and apoptosis in neuronal and myogenic cells. *Biochem. Biophys. Res.* 348, 787–793

Laliberte, R. E., Perregaux, D. G., Hoth, L. R., Rosner, P. J., Jordan, C. K., Peese, K. M., Eggler, J. F., Dombroski, M. A., Geoghegan, K. F., and Gabel, C. A. (2003) Glutathione *S*-transferase Omega 1-1 is a target of cytokine release-inhibitory drugs and may be responsible for their effect on interleukin-1β posttranslational processing. *J. Biol. Chem.* 278, 16567–16578

Li, H. M., Buczkowski, G., Mittapalli, O., Xie, J., Wu, J., Westerman, R.,

Schemerhorn, B. J., Murdock, L. L., and Pittendrigh, B. R. (2008) Transcriptomic profiles of *Drosophila melanogaster* third instar larval midgut and responses to oxidative stress. *Insect Mol. Biol.* 17, 325–339

Li, Y. J., Oliveira, S. A., Xu, P., Martin, E. R., Stenger, J. E., Scherzer, C. R., Hauser, M. A., Scott, W. K., Small, G. W., Nance, M. A., Watts, R. L., Hubble, J. P., Koller, W. C., Pahwa, R., Stern, M. B., Hiner, B. C., Jankovic, J., Goetz, C. G., Mastaglia, F., Middleton, L. T., Roses, A. D., Saunders, A. M., Schmechel, D. E., Gullans, S. R., Haines, J. L., Gilbert, J. R., Vance, J. M., Pericak-Vance, M. A., Hulette, C., and Welsh-Bohmer, K. A. (2003) Glutathione *S*-transferase Omega-1 modifies age-at-onset of Alzheimer disease and Parkinson disease. *Hum. Mol. Genet.* 12, 3259–3267

Li, Y. J., Scott, W. K., Zhang, L., Lin, P. I., Oliveira, S. A., Skelly, T., Doraiswamy, M. P., Welsh-Bohmer, K. A., Martin, E. R., Haines, J. L., Pericak-Vance, M. A., and Vance, J. M. (2006) Revealing the role of glutathione *S*-transferase Omega in age-at-onset of Alzheimer and Parkinson diseases. *Neurobiol. Aging* 27, 1087–1093

Matyunina, L. V., Bowen, N. J., and McDonald, J. F. (2008) LTR retrotransposons and the evolution of dosage compensation in *Drosophila*. *BMC Mol. Biol.* 9, 55

Mayr, J. A., Havlickova, V., Zimmermann, F., Magler, I., Kaplanova, V., Jesina, P., Pecinova, A., Nuskova, H., Koch, J., Sperl, W., and Houstek, J. (2010)

Mitochondrial ATP synthase deficiency due to a mutation in the ATP5E gene for the F1 ε subunit. *Hum. Mol. Genet.* 19, 3430–3439

Murzin, A. G., Brenner, S. A., Hubbard, T., and Chothia, C. (1995) SCOP: a structural classification of proteins database for the investigation of sequences and structures. *J. Mol. Biol.* 247, 536–540

Nagy, P., Lechte, T. P., Das, A. B., and Winterbourn, C. C. (2012) Conjugation of glutathione to oxidative tyrosine resides in peptides and proteins. *J. Biol. Chem.* E-published

Palacino, J. J., Sagi, D., Goldberg, M. S., Krauss, S., Motz, C., Wacker, M., Klose, J., and Shen, J. (2004) Mitochondrial association of alpha-synuclein causes oxidative stress. *Cell Mol. Life. Sci.* 65, 1272–1284

Park, J., Lee, S. B., Lee, S., Kim, Y., Song, S., Kim, S., Bae, E., Kim, J., Shong, M., Kim, J. M., and Chung, J. (2006) Mitochondrial dysfunction in *Drosophila* PINK1 mutants is complemented by parkin. *Nature* 441, 1157–1161

Pena, P., and Garesse, R. (1993) The β subunit of the *Drosophila melanogaster* ATP synthase. cDNA cloning, amino acid analysis, and identification of the protein in adult flies. *Biochem. Biophys. Res. Commun.* 195, 785–791

Pesah, Y., Pham, T., Burgess, H., Middlebrooks, B., Verstreken, P., Zhou, Y., Harding, M., Bellen, H., and Mardon, G. (2004) *Drosophila* parkin mutants have decreased mass and cell size and increased sensitivity to oxygen radical stress. *Development* 131, 2183–2194

Petit, A., Kawarai, T., Paitel, E., Sanjo, N., Maj, M., Scheid, M., Chen, F., Gu, Y., Hasegawa, H., Salehi-Rad, S., Wang, L., Rogaeva, E., Fraser, P., Robinson, B., St George-Hyslop, P., and Tandon, A. (2005) Wild-type PINK1 prevents basal and induced neuronal apoptosis, a protective effect abrogated by Parkinson disease-related mutations. *J. Biol. Chem.* 280, 34025–34032

Poole, A. C., Thomas, R. E., Andrews, L. A., McBride, H. M., Whitworth, A. J., and Pallanck, L. J. (2008) The PINK1/Parkin pathway regulates mitochondrial morphology. *Proc. Natl. Acad. Sci. U.S.A.* 105, 1638–1643

Ransen, H., Rossiter, L., Ortelli, F., Jensen, B., Wang, X., Roth, C. W., Collins, F. H., and Hemingway, J. (2001) Identification of a novel class of insect glutathione S-transferases involved in resistance to DDT in the malaria vector *Anopheles gambiae*. *Biochem. J.*359, 295–304

Ren, Y., Zhao, J., and Feng, J. (2003) Parkin binds to α/β tubulin and increases their ubiquitination and degradation. *J. Neurosci.* 23, 3316–3324

Reynaert, N. L., Van der Vliet, A., Guala, A. S., McGovern, T., Hristova, M., Pantano, C., Heintz, N. H., Heim, J., Ho, Y. S., Matthews, D. E., Wouters, E. F., and Janssen-Heininger, Y. M. (2006) Dynamic redox control of NF-κB through glutaredoxin-regulated S-glutathionylation of inhibitory κB kinase β. *Proc. Natl. Acad. Sci. U.S.A.* 103, 13086–13091

Rosing, J., Harris, D. A., Kemp, A., Jr., and Slater, E. C. (1975) Nucleotidebinding properties of native and cold-treated mitochondrial ATPase. *Biochim. Biophys. Acta* 376, 13–26

Sheehan, D., Meade, G., Foley, V. M., and Dowd, C. A. (2001) Structure, function, and evolution of glutathione transferases. Implications for classification of non-mammalian members of an ancient enzyme superfamily. *Biochem. J.* 360, 1–16

Shelton, M. D., Mieyal, J. J. (2008) Regulation by reversible S-glutathionylation: molecular targets implicated in inflammatory disease. *Mol. Cells* 25, 332–346

Shi, M., Bradner, J., Bammler, T. K., Eaton, D. L., Zhang, J., Ye, Z., Wilson, A. M., Montine, T. J., and Pan, C. (2009) Identification of glutathione *S*-transferase Pi as a protein involved in Parkinson disease progression. *Am. J. Pathol.* 175, 54–65

Shimura, H., Hattori, N., Kubo, S., Mizuno, Y., Asakawa, S., Minoshima, S., Shimizu, N., Iwai, K., Chiba, T., Tanaka, K., and Suzuki, T. (2000) Familial

Parkinson disease gene product, parkin, is a ubiquitin-protein ligase. *Nat. Genet.* 25, 302–305

Shimura, H., Schlossmacher, M. G., Hattori, N., Frosch, M. P., Trockenbacher, A., Schneider, R., Mizuno, Y., Kosik, K. L., and Selkoe, D. J. (2001) Ubiquitination of a new form of α-synuclein by parkin from human brain: implications for Parkinson's disease. *Science* 293, 263–269

Smeyne, M., Boyd, J., Raviie Shepherd, K., Jiao, Y., Pond, B. B., Hatler, M., Wolf, R., Henderson, C., and Smeyne, R. J. (2007) GST Pi expression mediates dopaminergic neuron sensitivity in experimental parkinsonism. *Proc. Natl. Acad. Sci. U.S.A.* 104, 1977–1982

Smith, W. W., Jiang, H., Pei, Z., Tanaka, Y., Morita, H., Sawa, A., Dawson, V. L., Dawson, T. M., and Ross, C. A. (2005) Endoplasmic reticulum stress and mitochondrial cell death pathways mediate A53T mutant α-synuclein-induced toxicity. *Hum. Mol. Genet.* 14, 3801–3811

Sørensen, J. G., Nielsen, M. M., Kruhøffer, M., Justesen, J., and Loeschcke, V. (2005) Full genome gene expression analysis of the heat stress response in *Drosophila* melanogaster. *Cell Stress Chaperones* 10, 312–328

Starke, D. W., Chock, P. B., and Mieyal, J. J. (2003) Glutathione-thiyl radical

scavenging and transferase properties of human glutaredoxin (thioltransferase). Potential role in redox signal transduction. *J. Biol. Chem.* 278, 14607–14613

Staropoli, J. F., McDermott, C., Martinat, C., Schulman, B., Demireva, E., and Abeliovich, A. (2003) Parkin is a component of an SCF-like ubiquitin ligase complex and protects postmitotic neurons from kainite excitotoxicity. *Neuron* 37, 735–749

Stroombergen, M. C., and Waring, R. H. (1999) Determination of glutathione *S*-transferase Mu and Theta polymorphisms in neurological disease. *Hum. Exp. Toxicol.* 18, 141–145

Svensson, M. J., and Larsson, J. (2007) Thioredoxin-2 affects lifespan and oxidative stress in *Drosophila*. *Hereditas.* 144, 25–32

Tain, L. S., Mortiboys, H., Tao, R. N., Ziviani, E., Bandmann, O., and Whitworth, A. J. (2009) Rapamycin activation of 4E-BP prevents parkinsonian dopaminergic neuron loss. *Nat. Neurosci.* 12, 1129–1135

Tew, K. D., and Townsend, D. M. (2011) Regulatory functions of glutathione *S*-transferase P1-1 unrelated to detoxification. *Drug Metab. Rev.* 43, 179–193

Townsend, D. M., Manevich, Y., He, L., Hutchens, S., Pazoles, C. J., and Tew, K. D. (2009) Novel role for glutathione *S*-transferase Pi. Regulator of protein *S*-

glutathionylation following oxidative and nitrosative stress. *J. Biol. Chem.* 284, 436–445

Trinh, K., Moore, K., Wes, P. D., Muchowski, P. J., Dey, J., Andrews, L., and Pallanck, L. J. (2008) Induction of the phase II detoxification pathway suppresses neuron loss in *Drosophila* models of Parkinson's disease. *J. Neurosci.* 28, 465–472

Tsuda, M., Ootaka, R., Ohkura, C., Kishita, Y., Seong, K. H., Matsuo, T., and Aigaki, T. (2010) Loss of Trx-2 enhances oxidative stress-dependent phenotypes in *Drosophila*. *FEBS Lett.* 584, 3398–3401

Tu, C. P. D., and Akgul, B. (2005) *Drosophila* glutathione S-transferases. *Methods Enzymol.* 401, 204–226

Valente, E. M., Abou-Sleiman, P. M., Caputo, V., Muqit, M. M., Harvey, K., Gispert, S., Ali, Z., Del Turco, D., Bentivoglio, A. R., Healy, D. G., Albanese, A., Nussbaum, R., Gonzalez-Maldonado, R., Deller, T., Salvi, S., Cortelli, P., Gilks, W. P., Latchman, D. S., Harvey, R. J., Dallapiccola, B., Auburger, G., and Wood, N. W. (2004) Hereditary early-onset Parkinson's disease caused by mutations in PINK1. *Science* 304, 1158–1160

Verstreken, P., Ly, C. V., Venken, K. J., Koh, T. W., Zhou, Y., and Bellen, H. J. (2005) Synaptic mitochondria are critical for mobilization of reserve pool vesicles at

Drosophila neuromuscular junctions. *Neuron* 47, 365–378

Walters, K. B., Grant, P., and Johnson, D. L. (2009) Evolution of the GST Omega gene family in 12 *Drosophila* species. *J. Hered.* 100, 742–753

Wang, C., Lu, R., Ouyang, X., Ho, M. W., Chia, W., Yu, F., and Lim, K. L. (2007) *Drosophila* overexpressing parkin R275W mutant exhibits dopaminergic neuron degeneration and mitochondrial abnormalities. *J. Neurosci.* 27, 8563–8570

Wang, H. Q., Xu, Y. X., Zhao, X. Y., Zhao, H., Yan, J., Sun, X. B., Guo, J. C., and Zhu, C. Q. (2009) Overexpression of F_1F_0-ATP synthasae α suppresses mutant huntingtin aggregation and toxicity *in vitro*. *Biochem. Biophys. Res. Commun.* 390, 1294–1298

Whitworth, A. J., Theodore, D. A., Greene, J. C., Benes, H., Wes, P. D., and Pallanck, L. J. (2005) Increased glutathione *S*-transferase activity rescues dopaminergic neuron loss in a *Drosophila* model of Parkinson's disease. *Proc. Natl. Acad. Sci. U.S.A.* 102, 8024–8029

Willingham, S., Outeiro, T. F., DeVit, M. J., Lindquist, S. L., and Muchowski, P. J. (2003) Yeast genes that enhance the toxicity of a mutant huntingtin fragment or α-synuclein. *Science* 302, 1769–1772

Yang, Y., Ouyang, Y., Yang, L., Beal, M. F., McQuibban, A., Vogel, H., and Lu, B. (2008) Pink1 regulates mitochondrial dynamics through interaction with the fission/fusion machinery. *Proc. Natl. Acad. Sci. U.S.A.* 105, 7070–7075

Yin, S., Li, X., Meng, Y., Finley, R. L., Jr., Sakr, W., Yang, H., Reddy, N., and Sheng, S. (2005) Tumor-suppressive maspin regulates cell response to oxidative stress by direct interaction with glutathione *S*-transferase. *J. Biol. Chem.* 280, 34985–34996

Zhang, Y., Gao, J., Chung, K. K., Huang, H., Dawson, V. L., and Dawson, T. M. (2000) Parkin functions as an E2-dependent ubiquitin-protein ligase and promotes the degradation of the synaptic vesicle-associated protein, CDCrel-1. *Proc. Natl. Acad. Sci. U.S.A.* 97, 13354–13359

국문초록

파킨슨병은 진행성 신경퇴행 질환이다. 상염색체 열성 유전되는 유전자, *parkin*, *PINK1*, *DJ-1* 유전자의 돌연변이는 이른 시기에 파킨슨병을 유발한다. 파킨슨병의 주요 증상들은 중뇌 흑색질의 도파민 분비 신경세포의 선택적이고 폭넓은 사멸로 인한 결과로 나타난다. 최근 연구들이 parkin과 PINK1이 미토콘드리아의 기능과 동역학을 조절하는데 중요한 역할을 하는 것을 보여주었다. 또한 *parkin* 또는 *PINK1* 유전자 결실 돌연변이는 예정된 세포사멸의 증가, 산화스트레스의 증가 그리고 비정상 단백질의 축적 등을 포함하는 여러 결함이 있는 표현형을 보여준다. 현재까지 많은 집약적인 연구들에도 불구하고 그 정확한 분자 기작은 여전히 거의 알려진 바 없다.

다기능 유전자족 중의 하나인 글루타치온-S-전이효소는 세포 내부독성물질과 세포 외부독성물질에 대한 해독에 관여한다. 글루타치온-S-전이효소의 새로운 종류인 글루타치온-S-전이효소 오메가는 thioredoxin과 glutaredoxin 효소를 연상하는 글루타치온-의존성 티올 전이효소와 글루타치온-의존성 디하이드로 아스코브산 환원효소 활성을 갖는다. 최근 연구에서 인간의 *GSTO* 유전자가 파킨슨병의 연령별 발병에 관련된다는 것을 보여주었다. 게다가 GSTO는 신경 퇴행성질환 발병 원인에 연관된 산화스트레스에 대항하여 세포를 보호한다. 비록 신경 퇴행성질환에 대한 GSTO의 기능 연구들이 다수 있었지만 파킨슨병 진행에 GSTO의 역할에 대해 알려진 바가 거의 없다.

이 논문에서 우리는 초파리 *parkin* 돌연변이에서 발현이 감소된 초파리 GSTO1의 발현회복으로 *parkin* 돌연변이의 표현형이 완화됨을 보였으며 초파리 *GSTO1*의 결핍이 *parkin* 돌연변이 표현형을 강화함을 보였다. 우리는 추가로 미토콘드리아 F_1F_0-ATP 합성효소 (Complex V)의 핵심요소인 ATP

중합효소 β 소단위체가 초파리 GSTO1의 생체 내 새로운 표적단백질임을 규명했다. 또한 우리는 ATP 중합효소 β 소단위체의 glutathionylation이 초파리 GSTO1에 의해 회복되고 *parkin* 돌연변이에서 초파리 GSTO1의 발현 증가로 미토콘드리아 F_1F_0-ATP 합성효소의 활성과 조립이 부분적으로 회복됨을 밝혔다. 추가적으로 우리는 파킨슨병 원인유전자 중 하나인 *PINK1* 유전자의 돌연변이에서도 ATP 중합효소 β 소단위체의 glutathionylation이 감소되어 있으며, 또한 초파리 GSTO1 발현 증가로 *PINK1* 돌연변이의 결함 표현형이 회복됨을 보였다. 이들 결과들은 초파리 GSTO1이 초파리모델에서 PINK1/Parkin 경로와 상호작용함을 의미한다.

결론적으로 본 연구의 결과는 *parkin* 돌연변이에서 ATP 합성효소 활성 조절함으로써 보호 역할을 하는 초파리 GSTO1의 새로운 기작을 제시하였고 파킨슨병에 대한 잠재적인 치료법 개발에 관한 통찰력을 제시하였다.

주요어: 파킨슨병; 글루타치온-S-전이효소 Omega (GSTO); glutathionylation; 미토콘드리아; 미토콘드리아 F_1F_0-ATP 합성효소; ATP 합성효소 β 소단위체; *Drosophila melanogaster*

학 번: 2004-20498